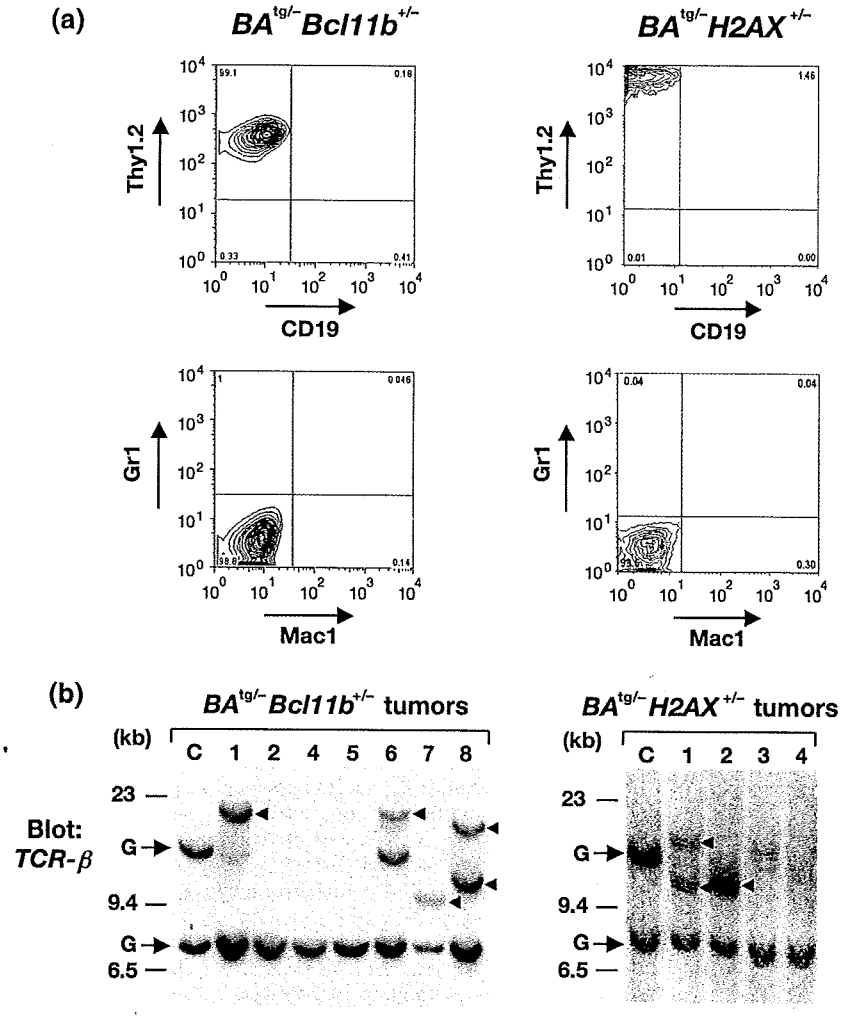

Fig. 3. Results of flow cytometric and Southern blot analyses of *BA*$^{tg/-}$*Bcl11b*$^{+/-}$ and *BA*$^{tg/-}$*H2AX*$^{+/-}$ leukemic mice. (a) Representative results of flow cytometry of leukemic cells that developed in *BA*$^{tg/-}$*Bcl11b*$^{+/-}$ (left panel) and *BA*$^{tg/-}$*H2AX*$^{+/-}$ (right panel) mice. In both samples, blast cells were positive for Thy1.2 but negative for CD19, Gr1, and Mac1, indicating that they were of T-cell phenotype. (b) Results of gene rearrangement analysis in tumors that developed in *BA*$^{tg/-}$*Bcl11b*$^{+/-}$ (left panel) and *BA*$^{tg/-}$*H2AX*$^{+/-}$ (right panel) mice. (c) DNA extracted from control thymus and thymomas that developed in *BA*$^{tg/-}$*Bcl11b*$^{+/-}$ (left panel) and *BA*$^{tg/-}$*H2AX*$^{+/-}$ (right panel) mice were digested with *Bam*HI and blotted with *TCR-β* probe. Germline and rearranged bands are indicated by arrows and arrowheads respectively. Molecular markers are shown on the left.

Table 2. Characteristics of p210BCR/ABL$^{tg/-}$ H2AX$^{+/-}$ leukemic mice

Mouse no.	Age at disease (months)	PB parameters			Macroscopic tumor sites	*TCRβ* status	p210BCR/ABL expression	H2AX expression	H2AX status
		WBC ($\times 10^3/\mu L$)	Hb (g/dL)	Plt ($\times 10^4/\mu L$)					
1	1.8	15.3	16.1	56.4	Thy, Spl	G/R	+	+	G/T
2	2.2	160.8	10.4	53.4	Thy, Spl, LN	G/R	+	–	G/T
3	2.5	128.4	12.0	90.9	Thy, Spl, LN	G/loss	+	–	G/T
4	2.8	84.7	12.4	36.0	Thy, Spl, LN	G/loss	+	+	G/T

G, germline; LN, lymph node; R, rearranged; Spl, spleen; T, targeted; Thy, thymus.

tissues was subjected to genomic PCR that distinguished the PCR product of the wild-type allele from that of the knockout allele (upper panels of Fig. 4c,d). The results showed that the wild-type *Bcl11b* allele-derived band was not amplified in the three samples without Bcl11b expression (no. 5, 6, and 8, lower panel of Fig. 4c), indicating that the absence of Bcl11b protein was attributed to the loss of the residual wild-type *Bcl11b* allele. In contrast, the PCR product from the wild-type *H2AX* allele was retained in the two samples lacking H2AX expression (no. 2 and 3 in the lower panel of Fig. 4d). Because the PCR primer set detecting the wild-type allele (P1 + P2) did not amplify the coding region of the *H2AX* gene (upper panel of Fig. 4d), we designed another primer set encompassing the *H2AX* exon. As *H2AX* is a single-exon gene,[10] this primer set (shown as P4 and P5 in the upper panel of Fig. 4d) amplified a part of the promoter and the whole coding region. The results showed that a PCR product of expected size was detected in all of the *BA*$^{tg/-}$*H2AX*$^{+/-}$ tumors (lower panel of Fig. 4d). To examine the possibility that subtle deletion and/or base substitution had occurred in this region, we sequenced the whole PCR product but could not detect any mutation (data not shown). In addition, Southern blotting using a 5′ external probe for the *H2AX* gene[10] did not show any gross rearrangement (data not shown). These results indicated that the structure of the *H2AX* gene was largely unaffected. We next examined H2AX mRNA expression in the *BA*$^{tg/-}$*H2AX*$^{+/-}$ tumors by northern blotting. Interestingly, as shown

doi: 10.1111/j.1349-7006.2009.01172.x

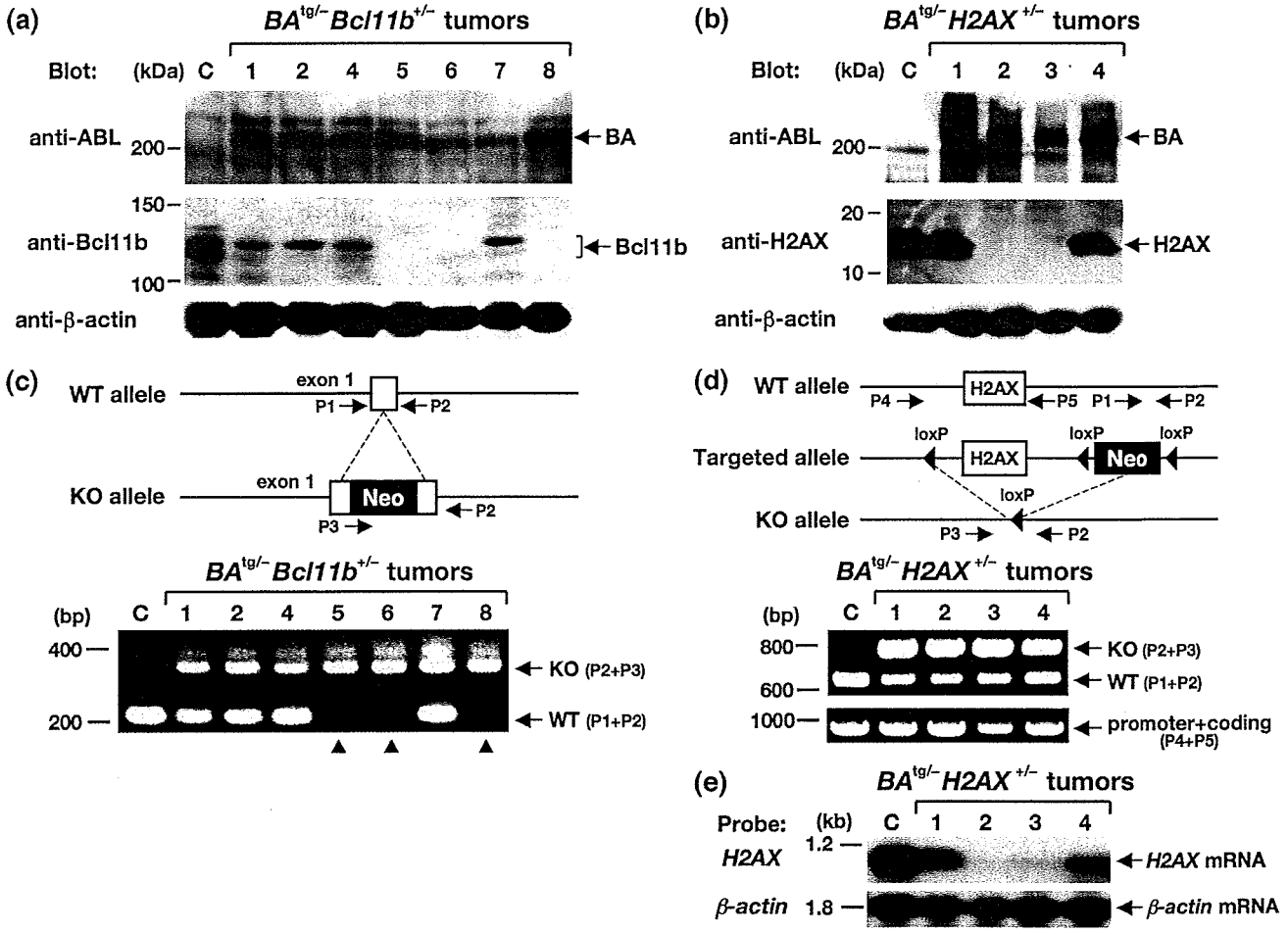

Fig. 4. Gene expression and PCR analyses of the tumors that developed in *BA*$^{tg/-}$*Bcl11b*$^{+/-}$ (left panels) and *BA*$^{tg/-}$*H2AX*$^{+/-}$ (right panels) mice. (a,b) Western blot analysis for the expression of p210BCR/ABL, Bcl11b, and H2AX proteins. Proteins extracted from a control (C) thymus and tumor tissues of *BA*$^{tg/-}$*Bcl11b*$^{+/-}$ (no. 1, 2, and 4–8) and *BA*$^{tg/-}$*H2AX*$^{+/-}$ mice (no. 1–4) were blotted with an anti-ABL antibody (upper panels) and anti-Bcl11b or anti-H2AX antibody (middle panels). The positions of p210BCR/ABL (BA), Bcl11b, and H2AX proteins are indicated by arrows. An anti-β-actin blot was carried out as an internal control (bottom panels). Protein markers are shown on the left. (c,d) Schematic illustrations of wild-type and targeted alleles for *Bcl11b* and *H2AX* genes (upper panels) and the resultant genomic PCR products (lower panels). DNA extracted from a control (C) thymus and tumor tissues of *BA*$^{tg/-}$*Bcl11b*$^{+/-}$ (no. 1, 2 and 4–8) and *BA*$^{tg/-}$*H2AX*$^{+/-}$ mice (no. 1–4) were amplified with sets of primers (P1 and P2 for wild-type [WT] alleles, P2 and P3 for knockout [KO] alleles, and P4 and P5 for a part of the promoter and the whole coding region of *H2AX*). The positions of primers are shown in the upper panels and WT- and KO-derived PCR products are indicated by arrows in the lower panels. Molecular markers are shown on the left. Samples without *Bcl11b* expression are indicated by arrowheads. *Neo*, neomycin resistance gene. (e) Expression of *H2AX* mRNA in *BA*$^{tg/-}$*H2AX*$^{+/-}$ tumors. RNA extracted from a control thymus (C) and tumor tissues of *BA*$^{tg/-}$*H2AX*$^{+/-}$ mice (no. 1–4) were hybridized with *H2AX* cDNA probe. *β-Actin* hybridization was carried out as an internal control. Molecular markers are shown on the left.

in Figure 4(e), no H2AX mRNA was detected in tumors lacking H2AX protein expression (no. 2 and 3). These results indicated that the absence of H2AX protein was not due to deletion or mutation in the *H2AX* gene but to a lack of mRNA expression.

Chromosomal abnormalities in the leukemic cells developed in *BA*$^{tg/-}$*H2AX*$^{+/-}$ mice. We finally examined the chromosomal status of the leukemic cells developed in *BA*$^{tg/-}$*H2AX*$^{+/-}$ mice, as previous reports demonstrated that haploinsufficiency and absence of H2AX led to increased incidence of chromosomal abnormalities.[14,15] In the four tumors that arose from *BA*$^{tg/-}$*H2AX*$^{+/-}$ mice, although two samples showed a normal karyotype (no. 1 and 4, data not shown), the other two samples (no. 2 and 3) that did not express H2AX protein (Fig. 4b) exhibited chromosomal aberrations. As shown in the left panel of Figure 5, sample no. 2 contained an additional chromosome (indicated by an arrowhead). In addition, as shown in the right panel of Figure 5, sample no. 3 exhibited deletions in the long arm of chromosome 6 and in the short arm of chromosome 13, and a breakage in chromosome 11 (indicated by arrows). These results suggested the possibility that the acquired loss of H2AX induced chromosomal instability and resulted in the chromosomal abnormalities observed in samples no. 2 and 3.

Discussion

Chronic myelogenous leukemia presents a paradigm for cancers that evolve through accumulation of genetic alterations. Generation of p210BCR/ABL initiates CML CP and additional genetic events progress the disease and develop CML BC.[1–3] Although chromosomal and molecular analyses revealed that various mechanisms are involved in the transition from CP to BC,[1–3] genes responsible for the evolution to BC have not fully been identified.

To elucidate the mechanisms underlying the disease evolution of CML, we have developed an *in vivo* model for CML in which expression of *p210BCR/ABL* induces CML CP, and additional

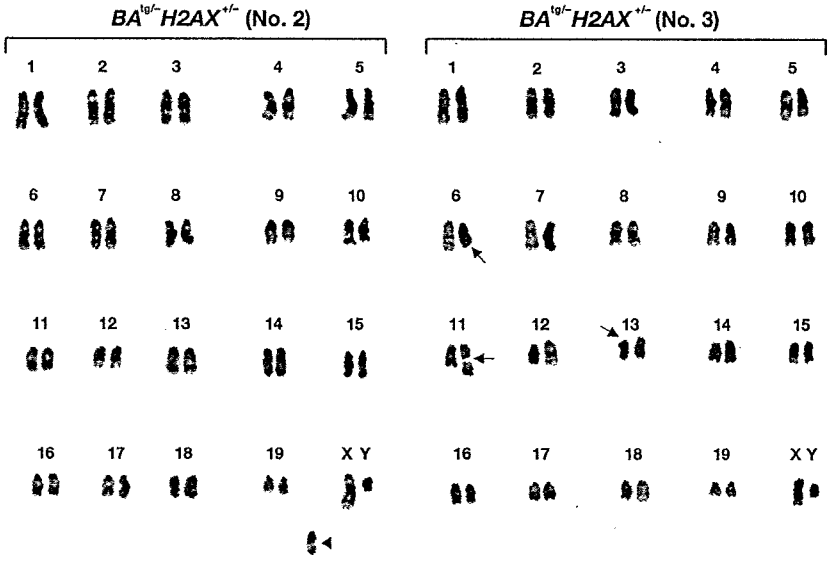

Fig. 5. Chromosomal abnormalities observed in two tumors (no. 2 and 3) that developed in *BA*$^{tg/-}$*H2AX*$^{+/-}$ mice. The additional chromosome in tumor no. 2 is indicated by an arrowhead, and deletion and breakage of the chromosomes in tumor no. 3 are indicated by arrows.

genetic alterations cooperate with *p210BCR/ABL* to progress the disease to CML BC.[4–7] Using this as a model system, we examined the possible contribution of haploisufficiency of *Bcl11b* and *H2AX* to CML BC, by crossing *p210BCR/ABL* transgenic mice (*BA*$^{tg/-}$) with *Bcl11b* heterozygotes (*Bcl11b*$^{+/-}$) and *H2AX* heterozygotes (*H2AX*$^{+/-}$).

Bcl11b encodes a zinc finger protein involved in thymocyte development and differentiation.[8] *Bcl11b* was originally identified as a gene homologous to *Bcl11a*, that was cloned from t(2;14)(p13;q32.3)-carrying malignant lymphomas,[16] and subsequently shown to be frequently deleted or mutated in radiation-induced thymoma in mice.[17] Conditional knockout analysis showed that acquired ablation of *Bcl11b* in thymocytes resulted in impaired positive selection, altered T-cell receptor signaling, and reduced survival.[18] In addition, a recent study revealed that *Bcl11b* is involved in human leukemia carrying inv(14)(q11.2q32.31), which resulted in generation of the *Bcl11b–TRDC* fusion transcript.[19] On the other hand, H2AX is a member of the histone H2A family and a constituent of the nucleosome, the basic subunit of chromatin.[9,20,21] In response to the DNA double-strand break, H2AX rapidly becomes phosphorylated on the serine residue located at the C-terminus to form γH2AX at the DNA double-strand break sites.[9,20,21] This event creates a focus in the nucleus, where DNA repair and chromatin remodeling proteins are recruited.[9,20,21] In human hematopoietic malignancies, a single nucleotide polymorphism upstream of the *H2AX* gene was found to be tightly associated with susceptibility to non-Hodgkin lymphoma.[22] These results indicated that *Bcl11b* and *H2AX* are functionally implicated in cell differentiation and chromosomal stability, respectively, and are involved in subsets of hematopoietic malignancies.

We found that 8 of 15 *BA*$^{tg/-}$*Bcl11b*$^{+/-}$ mice and 4 of 11 *BA*$^{tg/-}$*H2AX*$^{+/-}$ mice developed acute leukemia and died in a short period (Fig. 1). These results indicated that haploinsufficiency of *Bcl11b* and *H2AX* conferred a growth advantage to *p210BCR/ABL*-expressing hematopoietic cells and consequently induced acute leukemia. The blast cells were highly malignant, as evidenced by massive proliferation in the peripheral blood, destruction of the basic structure of the thymus, and marked infiltration in non-hematopoietic tissues (upper 3 panels of Fig. 2). Surface marker analysis showed that the leukemic cells were of T-cell phenotype and Southern blot analysis demonstrated that most of the tumors were clonal in origin (Fig. 3). As the bone marrow showed the typical picture of CML CP (bottom panels of Fig. 2), the leukemias that developed in *BA*$^{tg/-}$*Bcl11b*$^{+/-}$ and *BA*$^{tg/-}$*H2AX*$^{+/-}$ mice were considered to be CML T-cell BC rather than *de novo* T-cell malignancy.

Interestingly, protein analysis revealed that the expression of Bcl11b and H2AX was lost in several tumors that developed in the *BA*$^{tg/-}$*Bcl11b*$^{+/-}$ and *BA*$^{tg/-}$*H2AX*$^{+/-}$ mice (Fig. 4a,b, middle panels). These results strongly suggested that the expression of p210BCR/ABL rendered genetic instability in the hematopoietic cells and consequently lost the normal residual allele of *Bcl11b* and *H2AX*, as reported in our previous study.[5] Indeed, in *BA*$^{tg/-}$*Bcl11b*$^{+/-}$ tumors, genomic PCR analysis revealed that the wild-type *Bcl11b*-derived band was not amplified in tumors lacking Bcl11b expression (no. 5, 6, and 8 in the lower panel of Fig. 4c), indicating that loss of the normal *Bcl11b* allele was responsible for the lack of the protein product. In contrast, the tumor tissues with no H2AX expression in *BA*$^{tg/-}$*H2AX*$^{+/-}$ mice retained the normal *H2AX* allele, including the 3′ region, a part of the promoter region, and the whole coding region (no. 2 and 3 in the lower panels of Fig. 4d). Instead, we found that no H2AX mRNA was expressed in tumors lacking H2AX protein (no. 2 and 3 in the upper panel of Fig. 4e), which indicated that the absence of H2AX protein was due to the lack of H2AX mRNA expression. Although the mechanism underlying loss of the *H2AX* message in these tumors remains unclear, one possibility is that *p210BCR/ABL*-induced genetic alterations might have occurred in the other regions regulating *H2AX* transcription, such as the enhancer, which led to the loss of mRNA expression. Alternatively, p210BCR/ABL might have impaired the transcriptional machinery for H2AX mRNA in these tumors by an unknown mechanism. Taken together, our findings demonstrated that p210BCR/ABL induces loss of protein expression through several different mechanisms, including genomic instability and transcriptional inhibition.

It is to be noted that four *BA*$^{tg/-}$*Bcl11b*$^{+/-}$ and two *BA*$^{tg/-}$*H2AX*$^{+/-}$ leukemic mice retained Bcl11b and H2AX protein expression (no. 1, 2, 4, and 7 in the middle panel of Fig. 4a and no. 1 and 4 in the middle panel of Fig. 4b). Thus, the mechanism of how haploinsufficiency of these genes caused disease evolution is to be clarified. Although no obvious phenotypic abnormalities were found in *Bcl11b*$^{+/-}$ or *H2AX*$^{+/-}$ mice, previous studies demonstrated that both types of heterozygotes exhibit enhanced susceptibility to hematological malignancies on *p53*$^{+/-}$ and *p53*$^{-/-}$ backgrounds.[14,15,23] These results indicated that both genes function as a dosage-dependent tumor suppressor and their

doi: 10.1111/j.1349-7006.2009.01172.x

haploinsufficiency predisposes to cancer development in certain genetic backgrounds. Thus, it is possible that haploinsufficiency of *Bcl11b* and *H2AX* exerted its oncogenic potential in cooperation with *p210BCR/ABL*, conferred a growth advantage to *p210BCR/ABL*-expressing hematopoietic cells, and consequently developed CML BC. An alternative possibility is that because p210BCR/ABL is known to promote genetic instability,[3,5] altered expression of unknown genes synergized with haploinsufficient *Bcl11b* or *H2AX* in *p210BCR/ABL*-expressing hematopoietic cells, accelerated progression of CML, and eventually caused CML BC.

We finally examined the possible chromosomal abnormalities in the leukemic cells of $BA^{tg/-}$-$H2AX^{+/-}$ mice, as previous reports demonstrated that haploinsufficiency or deficiency of *H2AX* induced various chromosomal aberrations, especially on a $p53^{-/-}$ genetic background.[14,15] The results showed that two of four tumors exhibited chromosomal abnormalities, which were the presence of an additional chromosome, deletion in part of the long and short arms, and breakage in the body of several chromosomes (Fig. 5). Interestingly, $BA^{tg/-}$-$H2AX^{+/-}$ mice with these chromosomal abnormalities exhibited very high white blood cell (WBC) counts ($>1 \times 10^5/\mu L$, see the right top panel of Fig. 2 and Table 2), suggesting that these events conferred a marked proliferative ability to *p210BCR/ABL*-expressing hematopoietic cells and exhibited a very aggressive phenotype. We also examined the possible contribution of dysfunction of genes involved in error-prone non-homologous end joining, such as *DNA ligase IV* and *XRCC4*, by crossing $BA^{tg/-}$ with *DNA ligase IV* heterozygous mice and *XRCC4* heterozygous mice. However, we did not observe disease acceleration or CML BC in $BA^{tg/-}$-*DNA ligase* $IV^{+/-}$ or $BA^{tg/-}$-$XRCC4^{+/-}$ double transgenic mice (data not shown), suggesting the possibility that among DNA repair-associated genes, *H2AX* might play a unique role in the disease evolution of CML.

The CML BC observed in $BA^{tg/-}$-$Bcl11b^{+/-}$ and $BA^{tg/-}$-$H2AX^{+/-}$ mice were of T-cell phenotype. Although T-cell BC is frequently observed in mouse models for CML,[5,24] it is rarely detected in human clinical samples. The reason for this discrepancy is not clear but one possibility is that human CML originates from the acquisition of *p210BCR/ABL*-transformed hematopoietic stem cells and the T-cell lineage is rarely involved probably due to its prolonged life span, whereas every cell in transgenic (or knockout) mice inherently contains (or lacks) the target gene and T cells might be more susceptible to the target gene-induced oncogenic transformation than other types of hematopoietic cells.

It is intriguing to examine whether acquired expressional loss of *Bcl11b* and *H2AX* contributes to human CML BC. We examined *Bcl11b* and *H2AX* expression in several CML BC samples by RT-PCR but did not detect the absence of mRNA expression in either gene (Supporting Information Fig. S1), probably due to the limited number of samples available and a lack of T-cell crisis cases. Thus, an expanded study is required to clarify the clinical significance of dysfunction of these genes in the development of CML BC.

In the present report, we demonstrated that haploinsufficiency and acquired loss of protein expression of *Bcl11b* and *H2AX* cooperate with *p210BCR/ABL* and induce CML BC. Our findings demonstrated that altered expression of genes involved in cell differentiation or chromosomal integrity contributes to the development of CML BC, which provides insights into the molecular mechanisms underlying the disease evolution of CML.

Acknowledgments

This work was supported by a Grant-in-Aid from the Ministry of Education, Science, and Culture of Japan, a Grant-in-Aid for Cancer Research from the Ministry of Health, Labour, and Welfare of Japan (13-2), Research Grant of the Princess Takamatsu Cancer Research Fund, Astellas Research Foundation, YASUDA Medical Research Foundation, a Grant-in-Aid of The Japan Medical Association, and Japan Leukaemia Research Fund.

References

1 Calabretta B, Perrotti D. The biology of CML blast crisis. *Blood* 2004; **103**: 4010–22.
2 Ren R. Mechanisms of BCR-ABL in the pathogenesis of chronic myelogenous leukaemia. *Nat Rev Cancer* 2005; **5**: 172–83.
3 Melo JV, Barnes DJ. Chronic myeloid leukaemia as a model of disease evolution in human cancer. *Nat Rev Cancer* 2007; **7**: 441–53.
4 Honda H, Oda H, Suzuki T *et al.* Development of acute lymphoblastic leukemia and myeloproliferative disorder in transgenic mice expressing p210bcr/abl: a novel transgenic model for human Ph1-positive leukemias. *Blood* 1998; **91**: 2067–75.
5 Honda H, Ushijima T, Wakazono K *et al.* Acquired loss of p53 induces blastic transformation in p210bcr/abl-expressing hematopoietic cells: a transgenic study for blast crisis of human CML. *Blood* 2000; **95**: 1144–50.
6 Niki M, Cristofano DA, Zhao M *et al.* Role of Dok-1 and Dok-2 in leukemia suppression. *J Exp Med* 2004; **200**: 1689–95.
7 Mizuno T, Yamasaki N, Miyazaki K *et al.* Overexpression/enhanced kinase activity of BCR/ABL and altered expression of Notch1 induced acute leukemia in p210BCR/ABL transgenic mice. *Oncogene* 2008; **29**: 3465–74.
8 Wakabayashi Y, Watanabe H, Inoue J *et al.* Bcl11b is required for differentiation and survival of αβ T lymphocytes. *Nat Immunol* 2003; **4**: 533–9.
9 Bonner WM, Redon CE, Dickey JS *et al.* γH2AX and cancer. *Nat Rev Cancer* 2008; **8**: 957–67.
10 Bassing CH, Chua KF, Sekiguchi J *et al.* Increased ionizing radiation sensitivity and genomic instability in the absence of histone H2AX. *Proc Natl Acad Sci USA* 2002; **99**: 8173–8.
11 Miyazaki K, Kawamoto T, Tanimoto K, Nishiyama M, Honda H, Kato Y. Identification of functional hypoxia response elements in the promoter region of the DEC1 and DEC2 genes. *J Biol Chem* 2002; **277**: 47 014–21.
12 Honda H, Ohno S, Takahashi T, Takatoku M, Yazaki Y, Hirai H. Establishment, characterization, and chromosomal analysis of new leukemic cell lines derived from MT/p210bcr/abl transgenic mice. *Exp Hematol* 1998; **26**: 188–97.
13 Harada H, Harada Y, Tanaka H, Kimura A, Inaba T. Implications of somatic mutations in the AML1 gene in radiation-associated and therapy-related myelodysplastic syndrome/acute myeloid leukemia. *Blood* 2003; **101**: 673–80.
14 Bassing CH, Suh H, Ferguson DO *et al.* Histone H2AX: a dosage-dependent suppressor of oncogenic translocations and tumors. *Cell* 2003; **114**: 359–70.
15 Celeste A, Difilippantonio S, Difilippantonio MJ *et al.* H2AX haploinsufficiency modifies genomic stability and tumor susceptibility. *Cell* 2003; **114**: 371–83.
16 Satterwhite E, Sonoki T, Willis TG *et al.* The BCL11 gene family: involvement of BCL11A in lymphoid malignancies. *Blood* 2001; **98**: 3413–20.
17 Wakabayashi Y, Inoue J, Takahashi Y *et al.* Homozygous deletions and point mutations of the Rit1/Bcl11b gene in gamma-ray induced mouse thymic lymphomas. *Biochem Biophys Res Commun* 2003; **301**: 598–603.
18 Albu DI, Feng D, Bhattacharya D *et al.* BCL11B is required for positive selection and survival of double-positive thymocytes. *J Exp Med* 2008; **204**: 3003–15.
19 Przybylski GK, Dik WA, Wanzeck J *et al.* Disruption of the BCL11B gene through inv (14) (q11.2q32.31) results in the expression of BCL11B-TRDC fusion transcripts and is associated with the absence of wild-type BCL11B transcripts in T-ALL. *Leukemia* 2005; **19**: 201–8.
20 Riches LC, Lynch AM, Gooderham NJ. Early events in the mammalian response to DNA double-strand breaks. *Mutagenesis* 2008; **23**: 331–9.
21 Kinner A, Wu W, Staudt C, Iliakis G. c-H2AX in recognition and signaling of DNA double-strand breaks in the context of chromatin. *Nucl Acids Res* 2008; **36**: 5678–94.
22 Novik KL, Spinelli JJ, Macarthur AC *et al.* Genetic variation in H2AFX contributes to risk of non-Hodgkin lymphoma. *Cancer Epidemiol Biomarkers Prev* 2007; **16**: 1098–106.
23 Kamimura K, Ohi H, Kubota T *et al.* Haploinsufficiency of Bcl11b for suppression of lymphomagenesis and thymocyte development. *Biochem Biophys Res Commun* 2007; **355**: 538–42.
24 Gishizky ML, Johnson-White J, Witte ON. Efficient transplantation of BCR-ABL-induced chronic myelogenous leukemia-like syndrome in mice. *Proc Natl Acad Sci USA* 1993; **90**: 3755–9.

Supporting information

Additional Supporting Information may be found in the online version of this article:

Fig. S1. Expression of *Bcl11b* and *H2AX* in chronic myelogenous leukemia (CML) chronic phase (CP), CML blast crisis (BC), and normal bone marrow (BM). RNA extracted from one CML CP sample, four CML BC samples (two myeloid and two B-lymphoid), and one normal BM sample were subjected to RT-PCR for the expression of *Bcl11b* and *H2AX*. *β-Actin* RT-PCR was carried out as an internal control.

Please note: Wiley-Blackwell are not responsible for the content or functionality of any supporting materials supplied by the authors. Any queries (other than missing material) should be directed to the corresponding author for the article.

doi: 10.1111/j.1349-7006.2009.01172.x

Nutrition and Cancer, 60(5), 675–684
Copyright © 2008, Taylor & Francis Group, LLC
ISSN: 0163-5581 print / 1532-7914 online
DOI: 10.1080/01635580802008286

Routledge
Taylor & Francis Group

A Novel Prodrug of 4′-Geranyloxy-Ferulic Acid Suppresses Colitis-Related Colon Carcinogenesis in Mice

Shingo Miyamoto
Division of Food Science and Biotechnology, Graduate School of Agriculture, Kyoto University, Kyoto, Japan

Francesco Epifano
Dipartimento di Scienze del Farmaco, Università "G. D'Annunzio," Chieti, Italy

Massimo Curini and Salvatore Genovese
Dipartimento di Chimica e Tecnologia del Farmaco, Sezione di Chimica Organica, Università degli Studi di Perugia, Perugia, Italy

Mihye Kim, Rikako Ishigamori-Suzuki, Yumiko Yasui, Shigeyuki Sugie, and Takuji Tanaka
Department of Oncologic Pathology, Kanazawa Medical University, Ishikawa, Japan

The inhibitory effects of a novel prodrug, 3-(4′-geranyloxy-3′-methoxyphenyl)-2-*trans*-propenoyl-L-alanyl-L-proline (GAP), of the secondary metabolite 4′-geranyloxy-3′-methoxyphenyl)-2-*trans*-propenoic acid (4′-geranyloxy-ferulic acid), on colon carcinogenesis was investigated using an azoxymetahen (AOM)/dextran sodium sulfate (DSS) model. GAP was synthetically derived from ferulic acid. Male CD-1 (ICR) mice initiated with a single intraperitoneal injection of azoxymethane (10 mg/kg body weight) were promoted by 1% (wt/vol) DSS in drinking water for 7 days. They were then given modified AIN-76A diet containing 0.01% or 0.05% GAP for 17 wk. At Week 20, the development of colonic adenocarcinoma was significantly inhibited by GAP feeding at dose levels of 0.01% [60% incidence ($P = 0.0158$) with a multiplicity of and 1.13 ± 1.13 ($P < 0.05$)] and 0.05% [53% incidence ($P = 0.0057$) with a multiplicity of 0.08 ± 1.08 ($P < 0.01$)], when compared to the AOM/DSS group (95% incidence with a multiplicity of 3.10 ± 3.06). Dietary GAP modulated the mitotic and apoptotic indexes in the crypt cells and lowered 8-hydroxy-2′-deoxyguanosine (8-OHdG)-positive cells in the colonic mucosa. Urinary level of 8-OHdG was lowered by GAP feeding. Additionally, dietary GAP elevated the immunoreactivity of an inducible form of heme oxygenase 1 in the colonic mucosa. Our results indicate that GAP is able to inhibit colitis-related colon carcinogenesis by modulating proliferation and oxidative stress in mice.

Submitted 19 December 2007; accepted in final form 18 February 2008.

Address correspondence to Takuji Tanaka, Department of Oncologic Pathology, Kanazawa Medical University, 1-1 Daigaku, Uchinada, Ishikawa 920-0293, Japan. E-mail: takutt@kanazawa-med.ac.jp

INTRODUCTION

Colorectal cancer (CRC) is one of the leading causes of cancer deaths in the Western countries. Globally, the mortality of CRC was 655,000 deaths per year in 2005 (1). Inflammation was known to be linked with cancer development in several tissues (2). CRC is one of the most serious complications of inflammatory bowel disease (IBD), including ulcerative colitis and Crohn's disease. The risk of CRC increases with increasing extent and duration of the disease (3). For treatment or chemoprevention of IBD and IBD-related CRC, many drugs and chemopreventive agents were introduced (4). A large amount of the drugs are absorbed from the upper gastrointestinal tract, stomach, and small intestine and cause certain side effects. Therefore, it is preferable to deliver the drug site specifically to the colon.

Several synthetic or natural compounds exerting antioxidative and/or anti-inflammatory properties have been proposed as cancer chemopreventive agents (5–7). We previously reported that ferulic acid (R = H, Fig. 1a), abundant in edible plants, such as rice and black raspberries, is able to inhibit chemically induced carcinogenesis in rodents (8). Other investigators have reported data supporting our findings (9,10). A secondary metabolite biosynthetically derived from ferulic acid, 3-(4′-geranyloxy-3′-methoxyphenyl)-2-*trans*-propenoic acid (R = geranyl, Fig. 1a), is supposed to exert cancer chemopreventive effect (11).

Recently, novel natural and semisynthetic compounds with anti-inflammatory activity (12) have been reported to be effective chemopreventive agents against carcinogenesis in preclinical animal studies, such as collinin (7-geranyloxy-8-methoxy-coumarin) (13), auraptene (13,14) and the ethyl ester

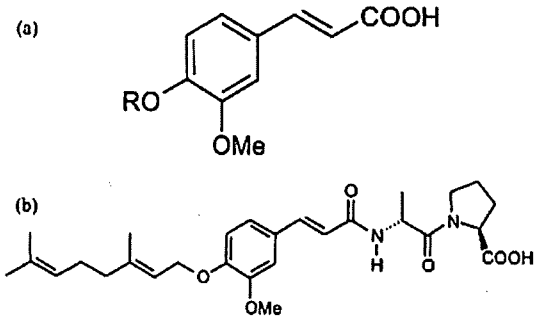

FIG. 1. Chemical structure of (a) ferulic acid. R = H and 3-(4-geranyloxy-3'-methoxyphenyl)-2-*trans*-propenoic acid. R = geranyl, and (b) 3-(4'-geranyloxy-3'-methoxyphenyl)-2-trans-propenoyl-L-alanyl-L-proline (GAP, molecular weight = 498.62).

of 3-(4'-geranyloxy-3'-methoxyphenyl)-2-*trans*-propenoic acid (EGMP) (15,16). Because inflammation is a universal and physiological response in the process of carcinogenesis (2,17–19), the in vivo and in vitro anti-inflammatory properties of these compounds have been demonstrated (20,21). Auraptene and collinin were reported to cause complete inhibition of platelet aggregation induced by arachidonic acid and platelet-activating factor in vitro (22), to act as good chemopreventers in colitis-related mouse colon tumorigenesis (13). In addition, our synthetic derivative, EGMP, has shown various interesting biological effects such as suppression of inducible nitric oxide (iNOS) and cyclooxygenase (COX)-2 protein expression in RAW 264.7 cells induced by lipopolysaccharide and interferon gamma (23) and colon and tongue cancer chemoprevention by dietary feeding in rats (15,16). Furthermore, some myo-inositol esters of 4'-geranoxy-ferulic acid have good inhibitory effects on phorbol ester-induced superoxide generation and Epstein-Barr virus activation (24). All these esters could be hydrolyzed to the parent acid once inside the cells. So the true active compound exerting the above-cited observed biological effects would be 3-(4'-geranoxy-3'-methoxyphenol)-2-*trans*-propenoic acid. Then, it could become a novel candidate as chemopreventive agent of various cancer types and as an anti-inflammatory compound. Pharmacological and chemical properties of the latter acid were recently reviewed (11). To achieve a novel approach in the prevention of CRC by drugs administered in diet, we carried out the synthesis of a novel prodrug, 3-(4'-geranyloxy-3'-methoxyphenyl)-2-*trans*-propenoyl-L-alanyl-L-proline (GAP, molecular weight = 498.62, Fig. 1b). This novel prodrug of 4'-geranyloxy-ferulic acid was structurally built to be hydrolized by intestinal angiotensin-converting enzyme; this enzyme is an exopeptidase that is quite abundant in the external side of the brush border of the epithelium of the small intestine, and its specificity is to hydrolize the last peptidic link in tripeptides in which +-Ala (or Gly) and L-pro occupy the second-last and last positions, respectively. Based on features of this prodrug, 3-(4'-geranyloxy-3'-methoxyphenyl)-2-*trans*-propenoic acid would be delivered in high concentration in the large bowel (25). Furthermore, its mechanism of activation would ensure chemical and enzymatic stability while passing through the stomach and small intestine by in vitro study (25).

For investigation of the pathogenesis (26–28) and chemoprevention (13,29) of inflammation-related CRC, our mouse model of inflammation related 2-stage colon carcinogenesis with a colonic carcinogen, and a colitis-inducing agent, dextran sodium sulfate (DSS) (15), is useful (30,31). In this model, the powerful tumor promoting effect of DSS is closely related to oxidative/nitrosative stress caused by DSS-induced colitis (26–28). This suggests that oxidative/nitrosative DNA damage by inflammation is involved in carcinogenesis, and thus it is important to control the events leading to inflammation-related carcinogenesis (17). In humans, oxidative stress also plays a key role in the pathogenesis of IBD-related intestinal damage (32). 8-Hydroxy-2'-deoxyguanosine (8-OHdG) production is induced by the oxidation of deoxyguanosine (dG), which is one of the components of DNA. Hydroxyl radicals (•OH) directly act on dG to form 8-OHdG. It is stable in humans and is excised by repair enzymes like 8-oxoguanine DNA glycosylase 1 and excreted in urine. 8-OHdG formation in DNA may also be related to tumorigenesis because many mutagens, tumor promoters, and carcinogens are known to generate oxygen radicals, and this generation of oxygen radicals in vivo is thought to be relevant to carcinogenesis (33). Elevation of urinary and tissue 8-OHdG levels are also known in IBD patients (32).

In the current study, we investigated whether dietary GAP exerts cancer chemopreventive ability in colitis-associated colon carcinogenesis using our mouse model (34). Also, effects of GAP on oxidative stress induced by azoxymetahen (AOM) and/or DSS were evaluated by measuring urinary level of 8-OHdG and immunohistochemical expression of 8-OHdG in the colonic mucosa. Additionally, we measured immunohistochemical expression of an important antioxidant enzyme, heme oxygenase (HO)-1, that is involved in the heme degradation process in the colonic mucosa because the significance of targeted induction of HO-1 as a strategy to achieve chemoprevention and chemoprotection is suggested (35).

MATERIAL AND METHODS

Animals, Chemicals, and Diets

Male Crj: CD-1 (ICR) mice (Charles River Japan, Tokyo, Japan), aged 5 wk, were used in this study. The animals were maintained in Kanazawa Medical University Animal Facility according to the Institutional Animal Care Guidelines. All animals were housed in plastic cages (5 mice/cage) with free access to tap water and a pelleted basal Charles River Formula-1 diet (Oriental Yeast Co., Ltd., Tokyo, Japan) during quarantine under controlled conditions of humidity (50 ± 10%), lightning (12-h light/dark cycle), and temperature (23°C ± 2°C). They were quarantined for 7 days after arrival and randomized by body

weight into experimental and control groups. A colonic carcinogen AOM was purchased from Sigma-Aldrich Chemical Co. (St. Louis, MO). DSS with a molecular weight of 36,000 to 50,000 was purchased from ICN Biochemicals (Aurora, OH). DSS for induction of colitis was dissolved in water at 1% (wt/vol). GAP was synthesized, as described previously (25). Experimental diets containing 0, 0.01, and 0.05% GAP in modified AIN-76A (36) were prepared weekly in our laboratory and stored in a cold room. Animals had access to food and water at all times. Food cups were replenished with fresh diet everyday. All handling and procedures were carried out in accordance with the Institutional Animal Care Guidelines.

Experimental Procedures

The Institutional Animal Care and Use Committee evaluated all animal procedures associated with the present study and assured that all proposed methods were appropriate.

A total of 60 male ICR mice were divided into 5 experimental and control groups. Mice in Groups 1 through 3 were initiated with AOM by single intraperitoneal injection (10 mg/kg body weight). Starting 1 wk after the injection, 1% DSS in drinking water was administrated to mice for 7 days and then followed without any further treatment for 18 wk. Mice of Group 1 were maintained on modified AIN-76A diet throughout the study. Mice of Groups 2 and 3 were fed modified AIN-76A diets containing 0.01% GAP (Group 2) and 0.05% GAP (Group 3) for 17 wk, respectively, starting 1 wk after the cessation of DSS exposure. Group 4 did not receive AOM and DSS and were fed AIN-76A diet containing 0.05% GAP. Group 5 was fed modified AIN-76A diet and served as an untreated control. At the end of study (Week 20), all mice were sacrificed by CO_2 asphyxiation. They underwent careful necropsy, with emphasis on the colon, liver, kidney, lung, and heart.

At necropsy, the colons were flushed with saline, excised, their length measured (from ileocecal junction to the anal verge), cut open longitudinally along the main axis, and then washed with saline. They were cut and fixed in 10% buffered formalin for at least 24 h. Histological examination was performed on paraffin-embedded sections after hematoxylin and eosin (H & E) staining. Colonic tumors were diagnosed according to the Ward's (37) description. In brief, if the tumors cells with tubular formation invaded the depth of submucosa, the tumor was diagnosed as adenocarcinoma. When the tumors cells with glandular structure did not invade the submucosa and compressed the surrounding crypts, the tumor was diagnosed as adenoma.

Scoring of Inflammation in the Large Bowel

Inflammation in the large bowel was scored on the H & E-stained sections. For scoring, large intestinal inflammation was graded according to the following morphological criteria (38): Grade 0, normal appearance; Grade 1, shortening and loss of the basal 1/3 of the actual crypts with mild inflammation in the mucosa; Grade 2, loss of the basal 2/3 of the crypts with moderate inflammation in the mucosa; Grade 3, loss of the entire crypts with severe inflammation in the mucosa and submucosa but with retainment of the surface epithelium; and Grade 4, presence of mucosal ulcer with severe inflammation (infiltration of neutrophils, lymphocytes, and plasma cells) in the mucosa, submucosa, muscularis propria, and/or subserosa. The scoring was made on the entire colon with or without proliferative lesions and expressed as a mean average score/mouse.

Counting Mitotic and Apoptotic Cells and Crypt Heights

To identify intramucosal apoptotic and mitotic cells in the crypts, paraffin-embedded sections from the distal colon were stained with H & E and evaluated under a light microscope for apoptotic and mitotic cells at a magnification of 400. Apoptotic cells were identified by cell shrinkage, homogeneous basophilic and condensed nuclei, nuclear fragments (apoptotic bodies), marked eosinophilic condensation of the cytoplasm, and sharply delineated cell borders surrounded with a clear halo (39). The apoptotic and mitotic indexes in the colonic crypts were determined on longitudinal sections that allowed evaluation of the whole crypt from the top to the base. One colonic section (from the distal part) per mouse was studied and scored. Randomly chosen crypts (28–56 crypts/colon) with well-oriented crypt structure from the mouth to the base were evaluated for counting apoptosis and mitosis. The apoptotic index (AI) and mitotic index (MI) nuclei were determined by dividing the total number of apoptotic or mitotic cells by the number of epithelial cells evaluated.

Immunohistochemistry of 8-OHdG and HO-1

Immunohistochemistry for 8-OHdG and HO-1 was performed on 4 μm-thick paraffin-embedded sections from the colons of mice in each group. The paraffin-embedded sections were heated for 30 min at 65°C, deparaffinized in xylene, and rehydrated through graded ethanol at room temperature. A 0.05 M Tris hydrochloride buffer (pH 7.6) was used to prepare solutions and for washes between various steps. Incubations were performed in a humidified chamber. Sections were treated for 40 min at room temperature, with 2% bovine serum albumin, and incubated overnight at 4°C with primary antibodies such as anti-8-OHdG mouse monoclonal antibody (diluted 1:100; Institute of Aging, Japan) and anti-HO-1 rabbit polyclonal antibody (diluted 1:200, SPA-896; StressGen Biotechnologies, Ann Arbor, MI). To reduce the nonspecific staining of mouse tissue by the mouse antibodies, a Mouse On Mouse immunoglobulin G blocking reagent (Vector Laboratories, Inc., Burlingame, CA) was applied. For 8-OHdG and HO-1 immunohistochemistry, normal rabbit serum was used to block background staining. Staining was performed using a DAKO En Vision kit (DAKO, Glostrup, Denmark) or Vectastain Elite ABC Kit (Vector Laboratories). At the last step, the sections were counterstained with hematoxylin. As a negative control, omission of the primary antibody was used. Two observers (T. Tanaka and S. Sugie) were

unaware of the treatment group to which the slide belonged and evaluated the immunoreactivity with grading between 0 and 5: 0 (<15% of the colonic mucosa examined shows positive reactivity), 1 (16–30% of the colonic mucosa examined shows positive reactivity), 2 (31–45% of the colonic mucosa examined shows positive reactivity), 3 (46–60% of the colonic mucosa examined shows positive reactivity), 4 (61–75% of the colonic mucosa examined shows positive reactivity), and 5 (>75% of the colonic mucosa examined shows positive reactivity).

Urinary 8-OHdG Analysis

To determine in vivo oxidative stress, urinary level of 8-OHdG was measured. One day before the sacrifice, 5 animals were selected randomly from each treatment group and placed individually into metabolic cages for urine collection. Urine was collected from each animal over a period of 3 h and frozen at −80°C until analysis. Urinary level of 8-OHdG was determined by competitive enzyme-linked immunoabsorbent assay (Genox, Baltimore, MD) and corrected for urinary creatinine concentrations.

Statistical Evaluation

Where applicable, data were analyzed using 1-way analysis of variance with Tukey–Kramer multiple comparisons test (GraphPad Instat version 3.05, GraphPad Softwear, San Diego, CA) with $P < 0.05$ as the criterion of significance. The Fisher's exact probability test was used for comparison of the incidence of lesions between 2 groups.

RESULTS

General Observation

During the experiment, some animals that received AOM/DSS (Group 1) or AOM/DSS→GAP (Groups 2 and 3) had bloody stool, but the symptom disappeared soon after stopping of DSS treatment. At Weeks 18 to 20, some mice of these groups had bloody stool again and anal prolapse with rectal tumor. There was no significant change between the experimental groups with regards to the parameters tested (body weight, liver weight, relative liver weight, spleen weight, kidney weight, and colon length). Further, no significant pathological alternations were found in these organs except the colon.

Pathological Findings

Macroscopically, nodular and polypoid colonic tumors were observed in the middle and distal colon of mice in Groups 1 through 3. These tumors were histopathologically tubule adenoma (Fig. 2A) or adenocarcinoma (well-/moderately differentiated; Fig. 2B). Some adenocarcinomas invaded into submucosa or serosa. Dysplastic crypts (Fig. 2C) were also observed surrounding neoplasms. Enlarged lymph nodes with inflammation were present around the large bowel with tumors. Mice of Groups 4 (GAP alone) and 5 (untreated) had no tumors in all the organs examined including the colon.

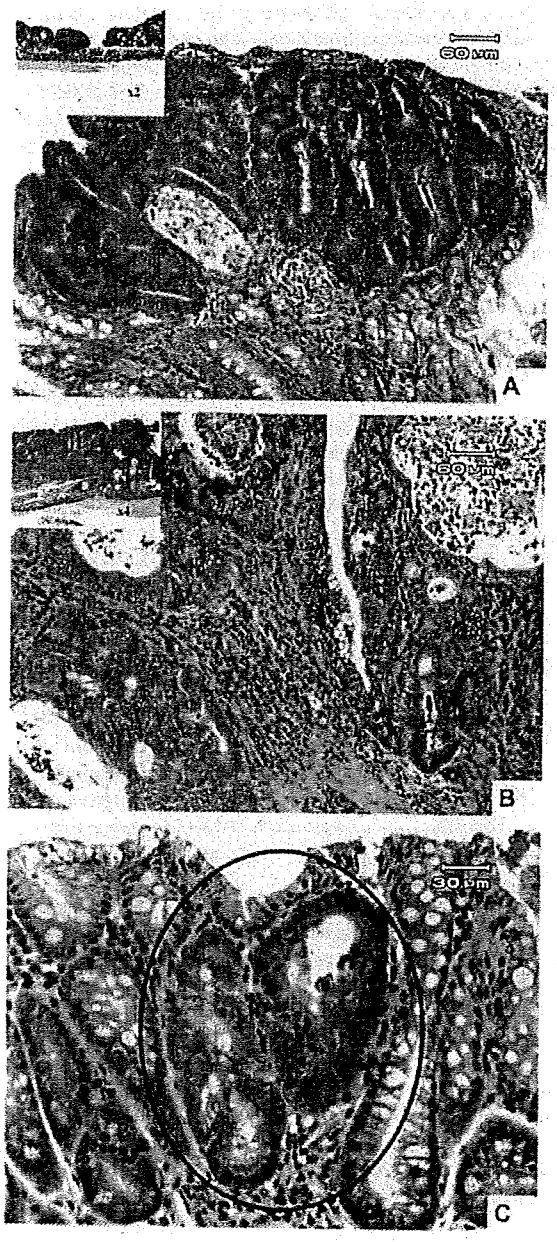

FIG. 2. Representative colonic lesions induced by azoxymetahen/dextran sodium sulfate in mice (Group 1): A: a tubular adenoma, B: a tubular adenocarcinoma with moderately differentiated, and C: dysplastic crypts (circled). Photos inserted in Fig. 2A and 2B are low power of views for each lesion (original magnifications are ×2 in 2A and ×4 in 2B). Figure represents hematoxylin and eosin stain, and bars inserted indicate magnification (μm).

TABLE 1
Incidence and Multiplicity of Colonic Tumors[a]

Group	Treatment	Incidence (No. of Mice With Tumors)			Multiplicity (No. of Tumors/Mouse)[b]		
		Total	AD	ADC	Total	AD	ADC
1	AOM/DSS (20)	20 (100%)	19 (95%)	19 (95%)	5.60 ± 4.81	2.50 ± 2.37	3.10 ± 3.06
2	AOM/DSS → 0.01% GAP (15)	10 (67%)[c]	8 (53%)[d]	9 (60%)[e]	2.33 ± 2.12[f]	1.20 ± 1.27	1.13 ± 1.13[f]
3	AOM/DSS → 0.05% GAP (15)	10 (67%)[c]	8 (53%)[d]	8 (53%)[d]	2.00 ± 2.10[f]	1.20 ± 1.37	0.80 ± 1.08[g]
4	0.05% GAP (5)	0 (0%)	0(0%)	0(0%)	0.00 ± 0.00	0.00 ± 0.00	0.00 ± 0.00
5	None (5)	0 (0%)	0(0%)	0(0%)	0.00 ± 0.00	0.00 ± 0.00	0.00 ± 0.00

[a]Abbreviations are as follows: AD, adenoma; ADC, adenocarcinoma; AOM, azoxymetahen; DSS, dextran sodium sulfate; GAP, 3-(4′-geranyloxy-3′-methoxyphenyl)-2-*trans*-propenoyl-L-alanyl-L-proline.

[b]Mean ± SD.

[c]Significantly different from the AOM/DSS group by Fisher's exact probability test, $P = 0.0002$.

[d]Significantly different from the AOM/DSS group by Fisher's exact probability test, $P = 0.0057$.

[e]Significantly different from the AOM/DSS group by Fisher's exact probability test, $P = 0.0158$).

[f]Significantly different from the AOM/DSS group 1-way analysis of variance (ANOVA) with Tukey–Kramer multiple comparisons test, $P < 0.05$.

[g]Significantly different from the AOM/DSS group 1-way ANOVA with Tukey–Kramer multiple comparisons test, $P < 0.01$.

The incidences and multiplicities of colon tumors are listed in Table 1. Group 1 (AOM + DSS) had 95% incidence of colon adenocarcinoma with a multiplicity of 3.10 ± 3.06. The incidences of colonic adenocarcinoma of Groups 2 (AOM/DSS→0.01% GAP, 60%) and 3 (AOM/DSS→0.05% GAP, 53%) were significantly smaller than that of Group 1 ($P = 0.0158$ and $P = 0.0057$, respectively). Also, the multiplicities of colonic adenocarcinoma of Groups 2 (1.13 ± 1.13, $P < 0.05$) and 3 (0.80 ± 1.08, $P < 0.01$) were significantly smaller than that of Group 1.

Inflammation Score in the Colon

Fig. 3A illustrates data on colonic inflammation scores at Week 20. The inflammation score of Group 1 (2.45 ± 0.89) was the greatest. The scores of Groups 2 (1.67 ± 0.82, $P < 0.05$) and 3 (1.07 ± 0.80, $P < 0.001$) were significantly lower than that of Group 1. Colonic inflammation in the mice of Groups 4 and 5 was slight, if present.

Indices of Mitosis and Apoptosis in Colonic Crypts

The data on the epithelial proliferative kinetics in the "normal appearing" distal colon are illustrated in Figs. 3B through 3D. As shown in Fig. 3B, the mean number of crypt cell MI of Groups 1 was significantly higher (4.33 ± 2.16, 2.37-fold increase; $P < 0.001$) than that of Group 5 (1.83 ± 1.60). The dietary administration of GAP (Groups 2 and 3) reduced the mean MI in a dose-dependent manner when compared to Group 1 (4.33 ± 2.16): 27% reduction by 0.01% GAP (Group 2, 3.17 ± 1.17, $P < 0.01$) and 54% reduction by 0.05% GAP (Group 3, 2.00 ± 0.89, $P < 0.001$). Feeding with 0.05% GAP alone (Group 4, 1.83 ± 1.17) did not affect the MI in the crypts when compared to an untreated control (Group 5, 1.83 ± 1.60). As indicated in Fig. 3C, the mean AI of group 1 (1.80 ± 0.84, $P < 0.05$) was significantly greater than that of Group 5 (1.20 ± 0.84). The values of Groups 2 (2.20 ± 0.84) and 3 (3.00 ± 0.71) were larger than that of Group 1, and the increase of Group 3 was statistically significant ($P < 0.001$). The mean AI of Groups 4 (1.40 ± 0.55) and 5 were comparable. As for the crypt column height (number of cells/crypt, Fig. 3D), the value in Group 1 (44.2 ± 4.97, $P < 0.001$), being the lowest among the groups, was significantly smaller than Group 5 (61.8 ± 8.76). The crypt column heights of Groups 2 (45.8 ± 6.06) and 3 (57.4 ± 12.6) were larger than Group 1, and the increase of Group 3 was statistically significant ($P < 0.001$). The value of Groups 4 (58.2 ± 5.81) and 5 were comparable.

Scores of 8-OHdG and HO-1 Immunohistochemistry

Mean scores of HO-1 and 8-OHdG immunohistochemistry are illustrated in Figs. 4A and 4B, respectively. The mean score of HO-1 immunohistochemical positivity of Group 1 (2.10 ± 0.88) was significantly greater than that of Group 5 (0.60 ± 0.89, $P < 0.05$; Fig. 4A). The score of Group 3 (3.40 ± 1.07) was significantly larger than Group 1. The value of Group 2 (3.00 ± 0.82) was greater than that of Group 1, but the increase was insignificant. As shown in Fig. 4B, the mean score of 8-OHdG immunohistochemical positivity of group 1 (3.90 ± 0.88) was significantly greater than that of Group 5 (0.40 ± 0.55, $P < 0.001$; Fig. 4B). The scores of Groups 2 (2.40 ± 0.52, $P < 0.001$) and 3 (1.80 ± 0.79, $P < 0.001$) were significantly lower than Group 1.

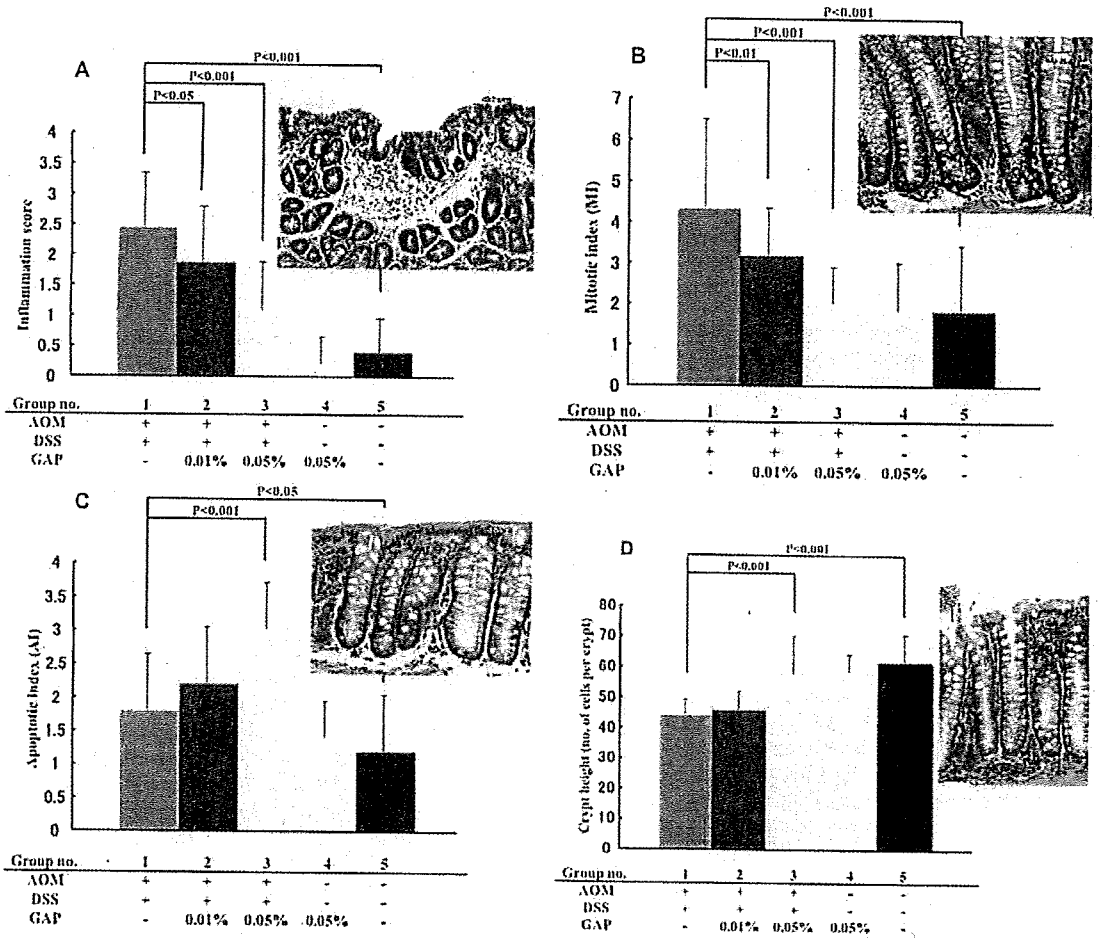

FIG. 3. A: Inflammation score (mean ± SD) of colon from each group. Photo shows inflammation score, Grade 2, in the colon of a mouse from Group 1; hematoxylin and eosin (H & E) stain; a bar inserted indicates magnification (μm). B: Mitotic index (MI, mean ± SD) of crypts of each group. For Fig. 3B photos, arrowheads in green are mitoses, and those in red are apoptotic nuclei or apoptotic bodies; H & E stain; a bar inserted indicates magnification (μm). C: Apoptotic index (AI, mean ± SD) of crypts of each group. For Fig. 3C photo, an arrowhead in green is a mitotic nucleus, and those in red are apoptotic nuclei or apoptotic bodies; H & E stain; a bar inserted indicates magnification (μm). D: Crypt height (number of cells per crypt, mean ± SD) of each group. For the Fig. 3D photo, arrowheads in green are mitoses, and an arrowhead in red is an apoptotic nucleus or apoptotic body; H & E stain; a bar inserted indicates magnification (μm). AOM, azoxymetahen; DSS, dextran sodium sulfate; GAP, 3-(4′-geranyloxy-3′-methoxyphenyl)-2-*trans*-propenoyl-L-alanyl-L-proline.

Urinary Level of 8-OHdG

Data on urinary 8-OHdG (ng/mg creatinine) are shown in Fig. 4C. The level of Group 1 (7.10 ± 1.60, $P < 0.001$) was significantly greater than that of Group 5 (3.20 ± 1.79). The values of Groups 2 (4.30 ± 1.57, $P < 0.01$) and 3 (3.70 ± 1.334, $P < 0.001$) were significantly smaller than that of Group 1. The levels of Groups 4 (4.00 ± 1.22) and 5 were comparable.

DISCUSSION

The results of this study clearly indicate that a novel prodrug of the already known colon cancer chemopreventive agent 3-(4′-geranyloxy-3′-methoxyphenyl)-2-*trans*-propenoic acid effectively inhibited AOM/DSS-induced, colitis-related, colonic carcinogenesis without any adverse effects in mice. Dietary feeding with GAP exerted its cancer chemopreventive ability by modulating cell proliferation, suppressing oxidative damage (tissue expression and urinary level of 8-OHdG), and enhancing an antioxidant enzyme, HO-1, in the inflamed colon. This is the first report showing that a prodrug, GAP, exerts cancer chemopreventive ability in colitis-related colon carcinogenesis.

The incidence and multiplicity of colonic tumors in the mice received AOM and 1% DSS in the current study were higher

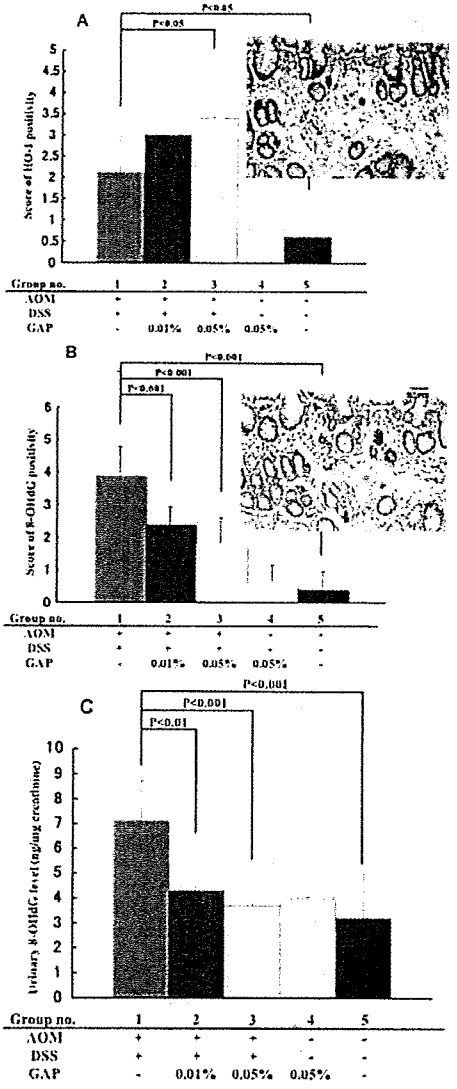

FIG. 4. A: Score (mean ± SD) of heme oxygenase (HO)-1 immunoreactivity. Photo shows strong HO-1 immunoreactivity (Grade 2) of colonic mucosa (same as an inset in Fig. 4) from a mouse of Group 1. Strong positive reaction is present in cryptal cells and inflammatory cells infiltrated into the inflamed colon; HO-1 immunohistochemistry; a bar inserted indicates magnification (μm). B: Score (mean ± SD) of 8-hydroxy-2′-deoxyguanosine (8-OHdG) immunoreactivity. Photo shows strong 8-OHdG immunoreactivity (Grade 3) of colonic mucosa from a mouse of Group 1. Strong positive reaction is present in inflammatory cells in the inflamed colon, and weak reaction is seen in the surface of crypt cells; 8-OHdG immunohistochemistry; a bar inserted indicates magnification (μm). C: Urinary 8-OHdG level (ng/mg creatinine, mean ± SD) of each group. The measurement was done by competitive enzyme-linked immunoabsorbent assay and corrected for urinary creatinine concentration. AOM, azoxymethane; DSS, dextran sodium sulfate; GAP, 3-(4′-geranyloxy-3′-methoxyphenyl)-2-*trans*-propenoyl-L-alanyl-L-proline.

than our previous dose-response study (40); this may be due to the difference of intake of 1% DSS-containing drinking water: 11.06 ± 0.05 ml/mouse/day in this study and 8.60 ± 0.94 ml/mouse/day in a previous investigation (40). Dietary GAP was able to modulate the endpoints measures in a dose-dependent manner, but the effects on tumor (total tumors and adenoma) multiplicity were comparable. The reason for this is unknown. However, the effects of GAP on the multiplicity of colonic adenocarcinoma suggest the inhibition of progression and the presence of dose-dependent efficacy. Therefore, we should determine the dose-dependency of the inhibition by GAP utilizing 3 or more doses in future studies.

Like ferulic acid (41), our data on 8-OHdG in the colon and urine suggests the antioxidative potential for GAP. Dietary administration of GAP effectively lowered the tissue expression of 8-OHdG in the inflamed colon as well as the urinary level of 8-OHdG. One of the markers of oxidative stress is 8-OHdG, which results from free radical damage to guanine (42). Elevated levels of 8-OHdG have been correlated with malignancy in the colon of rats (43) and humans (44). 8-Oxodeoxyguanosine, the tautomer of 8-OHdG, induces errors in DNA replication, specifically G-to-T transversions (45). Phenolic antioxidants in foods have been shown to reduce markers of oxidative stress and suppress carcinogenesis in certain tissues (46). For example, catechins in tea reduce urinary 8-OHdG content and are effective chemopreventives in the F344 model of colon carcinogenesis (47). In IBD patients, oxidative DNA damage and decrease in antioxidant activity are known (32). We previously reported increased oxidative damage in the inflamed colon of mice treated with DSS (26–28), and modulation of oxidative damage could prevent cancer occurrence (13,29). As found in a phase IIa clinical chemoprevention trial with green tea polyphenols in which urinary 8-OHdG can be monitored to determine oxidative stress condition (48), urinary concentration of 8-OHdG serves as a practical biomarker of oxidative DNA damage in preclinical animal studies.

In the current study, the treatment with GAP in diet significantly lowered colonic inflammation induced by DSS. Because chronic inflammation involves in carcinogenesis, suppression of chronic inflammation through modulation of expression of several pro-inflammatory gene products that mediate a critical role in several events of carcinogenesis may result in cancer chemoprevention (49). Ferulic acid and EGMP have anti-inflammatory effects and inhibition of iNOS expression and thereby suppress carcinogenesis (8,15,23). In fact, our recent study demonstrated that modulation of inflammation and expression of COX-2 and iNOS in the colon contributes to suppression of colitis-related colon carcinogenesis (50). Because several molecular targets for suppression of inflammation-associated carcinogenesis were proposed (51), further studies are warranted for detailed mechanisms by which GAP inhibits inflammation-related carcinogenesis.

Interesting findings observed in this study are that GAP treatment enhanced HO-1 expression in the colon of mice that

received AOM/DSS. HO-1 participates in endogenous cellular defense against oxidative stress (52). HO-1 confers cytoprotection against injury in a variety of organs and tissues where inflammatory processes are implicated. HO plays a central role in heme metabolism (52). At the same time, it protects cells from injury evoked by various oxidative stresses. HO-1 expression is carefully controlled in vivo with regard to its location and the magnitude. Furthermore, it was recently shown that HO-1 is involved in the immune regulation (53). These findings suggest HO-1 protein in vivo as a novel therapeutic intervention to control various forms of inflammatory disorders. Additionally, HO-1 is reported to inhibit inflammation through mitogen-activated protein kinase (MAPK) activation by induction of CO (54). The strategy that cell injury caused by oxidative stress and subsequent inflammatory condition are reduced and treated by induction of HO-1 expression is sound. However, because HO-1 is an inducible enzyme, we should control the expression quantitatively and with time. Several dietary constituents can modulate HO-1 expression (55). In addition to in vitro studies using known chemopreventive agents (56), there is an in vivo cancer chemoprevention study in which sulforaphane inhibits rat mammary carcinogenesis by induction of HO-1 (57). Upregulation of HO-1 by quercetin protects human hepatocytes from ethanol-induced oxidative stress via the MAPK/Nrf2 pathways (58). Also, Nrf2-dficient mice are susceptible to DSS-induced colitis (59). Therefore, safer natural compounds and their prodrug, such as GAP, may be used for prevention of inflammation-related cancer development.

When compared to the inhibitory effects of different chemicals on the multiplicity of colonic adenocarcinoma using this animal model, inhibitory potency was in the following order: ursodeoxycholic acid (29) > nimesulide (50) > collonin (13) > auraptene (13) > GAP (this study) > sulfasalazine (29) > pitavastatin (38) > troglitazone (50) > bezafibrate (50). However, we should consider the findings were observed in different experimental conditions such as dose of DSS and test chemicals and duration of exposure of chemicals. In addition, we need future experiments to check the effect of GAP on the kinetics of colon cancer development in our model system.

In conclusion, a novel prodrug of 3-(4′-geranyloxy-3′-methoxyphenyl)-2-*trans*-propenoic acid, resulting from the conjugation of this acid to the dipeptide L-Ala-L-Pro, is effective in inhibiting colon cancer development in a 2-stage, colitis-related, mouse colon carcinogenesis through modulation of inflammation, oxidative stress, and cell proliferation in the inflamed colon of mice that received AOM and DSS. Our findings support the development of novel, site-specifically delivered prodrugs for colon cancer prevention in the inflamed colon.

ACKNOWLEDGMENTS

This work was supported in part by a Grant-in-Aid for Cancer Research, for the Third-Term Comprehensive 10-Year Strategy for Cancer Control from the Ministry of Health, Labour and Welfare of Japan; a Grant-in-Aid (No. 18592076 to T. Tanaka, 17015016 to T. Tanaka, and 18880030 to Y. Yasui) for Scientific Research from the Ministry of Education, Culture, Sports, Science and Technology of Japan; and a grant (H2007–12 to T. Tanaka and S2006–9 to Y. Yasui) for the Project Research from the High-Technology Center of Kanazawa Medical University. We also thank Italian Ministero dell'Istruzione, Università e Ricerca (MIUR) for financial support for the synthesis of the title prodrug.

REFERENCES

1. Centre WM: Cancer. In *Fact sheet No. 297*. Geneva, Switzerland: WHO, 2006.
2. Balkwill F and Mantovani A: Inflammation and cancer: back to Virchow? *Lancet* **357**, 539–545, 2001.
3. Rubin DT and Parekh N: Colorectal cancer in inflammatory bowel disease: molecular and clinical considerations. *Curr Treat Options Gastroenterol* **9**, 211–220, 2006.
4. Chan EP and Lichtenstein GR: Chemoprevention: risk reduction with medical therapy of inflammatory bowel disease. *Gastroenterol Clin North Am* **35**, 675–712, 2006.
5. Tanaka T: Effect of diet on human carcinogenesis. *Crit Rev Oncol Hematol* **25**, 73–95, 1997.
6. Tanaka T: Chemoprevention of human cancer: biology and therapy. *Crit Rev Oncol Hematol* **25**, 139–174, 1997.
7. Aggarwal BB, Ichikawa H, Garodia P, Weerasinghe P, Sethi G, et al.: From traditional Ayurvedic medicine to modern medicine: identification of therapeutic targets for suppression of inflammation and cancer. *Expert Opin Ther Targets* **10**, 87–118, 2006.
8. Tanaka T, Kojima T, Kawamori T, Wang A, Suzui M, et al.: Inhibition of 4-nitroquinoline-1-oxide-induced rat tongue carcinogenesis by the naturally occurring plant phenolics caffeic, ellagic, chlorogenic, and ferulic acids. *Carcinogenesis* **14**, 1321–1325, 1993.
9. Hirose M, Takahashi S, Oguwa K, Futakuchi M, Shirai T, et al.: Chemoprevention of heterocyclic amine-induced carcinogenesis by phenolic compounds in rats. *Cancer Lett* **143**, 173–178, 1999.
10. Hudson EA, Dinh PA, Kokubun T, Simmonds MS, and Gescher A: Characterization of potentially chemopreventive phenols in extracts of brown rice that inhibit the growth of human breast and colon cancer cells. *Cancer Epidemiol Biomarkers Prev* **9**, 1163–1170, 2000.
11. Curini M, Epifano F, Genovese S, Marcotullio MC, and Menghini L: 3-(4′-geranyloxy-3′-methoxyphenyl)-2-trans propenoic acid: a novel promising cancer chemopreventive agent. *Anticancer Agents Med Chem* **6**, 571–577, 2006.
12. Curini M, Epifano F, Maltese F, Marcotullio MC, Tubaro A, et al.: Synthesis and anti-inflammatory activity of natural and semisynthetic geranyloxycoumarins. *Bioorg Med Chem Lett* **14**, 2241–2243, 2004.
13. Kohno H, Suzuki R, Curini M, Epifano F, Maltese F, et al.: Dietary administration with prenyloxycoumarins, auraptene and collinin, inhibits colitis-related colon carcinogenesis in mice. *Int J Cancer* **118**, 29336–2942, 2006.
14. Tanaka T, Kawabata K, Kakumoto M, Hara A, Murakami A, et al.: Citrus auraptene exerts dose-dependent chemopreventive activity in rat large bowel tumorigenesis: the inhibition correlates with suppression of cell proliferation and lipid peroxidation and with induction of phase II drug-metabolizing enzymes. *Cancer Res* **58**, 2550–2556, 1998.
15. Tanaka T, Kohno H, Nomura E, Taniguchi H, Tsuno T, et al.: A novel geranylated derivative, ethyl 3-(4′-geranyloxy-3′-methoxyphenyl)-2-propenoate, synthesized from ferulic acid suppresses carcinogenesis and inducible nitric oxide synthase in rat tongue. *Oncology* **64**, 166–175, 2003.
16. Han BS, Park CB, Takasuka N, Naito A, Sekine K, et al.: A ferulic acid derivative, ethyl 3-(4′-geranyloxy-3-methoxyphenyl)-2-propenoate, as

a new candidate chemopreventive agent for colon carcinogenesis in the rat. *Jpn J Cancer Res* **92**, 404–409, 2001.
17. Ohshima H, Tazawa H, Sylla BS, and Sawa T: Prevention of human cancer by modulation of chronic inflammatory processes. *Mutat Res* **591**, 110–122, 2005.
18. Philip M, Rowley DA, and Schreiber H: Inflammation as a tumor promoter in cancer induction. *Semin Cancer Biol* **14**, 433–439, 2004.
19. Surh YJ, Kundu JK, Na HK, and Lee J: Redox-sensitive transcription factors as prime targets for chemoprevention with anti-inflammatory and antioxidative phytochemicals. *J Nutr* **135**(12 Suppl), 2993S–3001S, 2005.
20. Murakami A, Nakamura Y, Ohto Y, Yano M, Koshiba T, et al.: Suppressive effects of citrus fruits on free radical generation and nobiletin, an anti-inflammatory polymethoxyflavonoid. *Biofactors* **12**, 187–192, 2000.
21. Murakami A, Nakamura Y, Tanaka T, Kawabata K, Takahashi D, et al.: Suppression by citrus auraptene of phorbol ester-and endotoxin-induced inflammatory responses: role of attenuation of leukocyte activation. *Carcinogenesis* **21**, 1843–1850, 2000.
22. Chen IS, Lin YC, Tsai IL, Teng CM, Ko FN, et al.: Coumarins and antiplatelet aggregation constituents from *Zanthoxylum schinifolium*. *Phytochemistry* **39**, 1091–1097, 1995.
23. Murakami A, Kadota M, Takahashi D, Taniguchi H, Nomura E, et al.: Suppressive effects of novel ferulic acid derivatives on cellular responses induced by phorbol ester, and by combined lipopolysaccharide and interferon-gamma. *Cancer Lett* **157**, 77–85, 2000.
24. Hosoda A, Nomura E, Murakami A, Koshimizu K, Ohigashi H, et al.: Synthesis of feruloyl-myo-insitol derivatives and their inhibitory effects on phorbol ester-induced superoxide generation and Epstein-Barr virus activation. *Bioorg Med Chem* **10**, 1855–1863, 2002.
25. Curini M, Epifano F, and Genovese S: Synthesis of a novel prodrug of 3-(4'-geranyloxy-3'-methoxyphenyl)-2-trans-propenoic acid for colon delivery. *Bioorg Med Chem Lett* **15**, 5049–5052, 2005.
26. Suzuki R, Kohno H, Sugie S, Nakagama H, and Tanaka T: Strain differences in the susceptibility to azoxymethane and dextran sodium sulfate-induced colon carcinogenesis in mice. *Carcinogenesis* **27**, 162–169, 2006.
27. Suzuki R, Kohno H, Sugie S, and Tanaka T: Sequential observations on the occurrence of preneoplastic and neoplastic lesions in mouse colon treated with azoxymethane and dextran sodium sulfate. *Cancer Sci* **95**, 721–727, 2004.
28. Suzuki R, Miyamoto S, Yasui Y, Sugie S, and Tanaka T: Global gene expression analysis of the mouse colonic mucosa treated with azoxymethane and detran sodium sulfate. *BMC Cancer* **7**, 84, 2007.
29. Kohno H, Suzuki R, Yasui Y, Miyamoto S, Wakabayashi K, et al.: Ursodeoxycholic acid versus sulfasalazine in colitis-related colon carcinogenesis in mice. *Clin Cancer Res* **13**, 2519–2525, 2007.
30. Tanaka T, Suzuki R, Kohno H, Sugie S, Takahashi M, et al.: Colonic adenocarcinomas rapidly induced by the combined treatment with 2-amino-1-methyl-6-phenylimidazo[4,5-*b*]pyridine and dextran sodium sulfate in male ICR mice possess beta-catenin gene mutations and increases immunoreactivity for beta-catenin, cyclooxygenase-2 and inducible nitric oxide synthase. *Carcinogenesis* **26**, 229–238, 2005.
31. Tanaka T, Kohno H, Suzuki R, Hata K, Sugie S, et al.: Dextran sodium sulfate strongly promotes colorectal carcinogenesis in Apc(Min/+) mice: inflammatory stimuli by dextran sodium sulfate results in development of multiple colonic neoplasms. *Int J Cancer* **118**, 25–34, 2006.
32. D'Inca R, Cardin R, Benazzato L, Angriman I, Martines D, et al.: Oxidative DNA damage in the mucosa of ulcerative colitis increases with disease duration and dysplasia. *Inflamm Bowel Dis* **10**, 23–27, 2004.
33. Kasai H, Crain PF, Kuchino Y, Nishimura S, Ootsuyama A, et al.: Formation of 8-hydroxyguanine moiety in cellular DNA by agents producing oxygen radicals and evidence for its repair. *Carcinogenesis* **7**, 849–851, 1986.
34. Tanaka T, Kohno H, Suzuki R, Yamada Y, Sugie S, et al.: A novel inflammation-related mouse colon carcinogenesis model induced by azoxymethane and dextran sodium sulfate. *Cancer Sci* **94**, 965–973, 2003.
35. Prawan A, Kundu JK, and Surh YJ: Molecular basis of heme oxygenase-1 induction: implications for chemoprevention and chemoprotection. *Antioxid Redox Signal* **7**, 1688–1703, 2005.
36. Rao CV, Wang CQ, Simi B, Rodriguez JG, Cooma I, et al.: Chemoprevention of colon cancer by a glutathione conjugate of 1,4-phenylenebis(methylene)selenocyanate, a novel organoselenium compound with low toxicity. *Cancer Res* **61**, 3647–3652, 2001.
37. Ward JM: Morphogenesis of chemically induced neoplasms of the colon and small intestine in rats. *Lab Invest* **30**, 505–513, 1974.
38. Yasui Y, Suzuki R, Miyamoto S, Tsukamoto T, Sugie S, et al.: A lipophilic statin, pitavastatin, suppresses inflammation-associated mouse colon carcinogenesis. *Int J Cancer* **121**, 2331–2339, 2007.
39. Wyllie AH, Kerr JF, and Currie AR: Cell death: the significance of apoptosis. *Int Rev Cytol* **68**, 251–306, 1980.
40. Suzuki R, Kohno H, Sugie S, and Tanaka T: Dose-dependent promoting effect of dextran sodium sulfate on mouse colon carcinogenesis initiated with azoxymethane. *Histol Histopathol* **20**, 483–492, 2005.
41. Ogiwara T, Satoh K, Kadoma Y, Murakami Y, Unten S, et al.: Radical scavenging activity and cytotoxicity of ferulic acid. *Anticancer Res* **22**, 2711–2717, 2002.
42. Floyd RA: The role of 8-hydroxyguanosine in carcinogenesis. *Carcinogenesis* **11**, 1447–1450, 1990.
43. Harris GK, Gupta A, Nines RG, Kresty LA, Habib SG, et al.: Effects of lyophilized black raspberries on azoxymethane-induced colon cancer and 8-hydroxy-2'-deoxyguanosine levels in the Fischer 344 rat. *Nutr Cancer* **40**, 125–133, 2001.
44. Weiss JM, Goode EL, Ladiges WC, and Ulrich CM: Polymorphic variation in hOGG1 and risk of cancer: a review of the functional and epidemiologic literature. *Mol Carcinogenesis* **42**, 127–141, 2005.
45. Shibutani S, Takeshita M, and Grollman AP: Insertion of specific bases during DNA synthesis past the oxidation-damaged base 8-oxodG. *Nature* **349**, 431–434, 1991.
46. Tanaka T, Miyamoto S, Suzuki R, and Yasui Y: Chemoprevention of colon carcinogenesis by dietary non-nutritive compounds. *Curr Top Neutraceutical Res* **4**, 127–152, 2006.
47. Matsumoto H, Yamane T, Inagake M, Nakatani H, Iwati Y, et al.: Inhibition of mucosal lipid hyperoxidation by green tea extract in 1,2-dimethylhydrazine-induced rat colonic carcinogenesis. *Cancer Lett* **104**, 205–209, 1996.
48. Luo H, Tang L, Tang M, Billam M, Huang T, et al.: Phase IIa chemoprevention trial of green tea polyphenols in high-risk individuals of liver cancer: modulation of urinary excretion of green tea polyphenols and 8-hydroxydeoxyguanosine. *Carcinogenesis* **27**, 262–268, 2006.
49. Aggarwal BB, Shishodia S, Sandur SK, Pandey MK, and Sethi G: Inflammation and cancer: how hot is the link? *Biochem Pharmacol* **72**, 1605–1621, 2006.
50. Kohno H, Suzuki R, Sugie S, and Tanaka T: Suppression of colitis-related mouse colon carcinogenesis by a COX-2 inhibitor and PPAR ligands. *BMC Cancer* **5**, 46, 2005.
51. Aggarwal BB and Shishodia S: Molecular targets of dietary agents for prevention and therapy of cancer. *Biochem Pharmacol* **71**, 1397–1421, 2006.
52. Maines MD and Gibbs PE: 30 some years of heme oxygenase: from a "molecular wrecking ball" to a "mesmerizing" trigger of cellular events. *Biochem Biophys Res Commun* **338**, 568–577, 2005.
53. Willis D, Moore AR, Frederick R, and Willoughby DA: Heme oxygenase: a novel target for the modulation of the inflammatory response. *Nat Med* **2**, 87–90, 1996.

54. Otterbein LE, Otterbein SL, Ifedigbo E, Liu F, Morse DE, et al.: MKK3 mitogen-activated protein kinase pathway mediates carbon monoxide-induced protection against oxidant-induced lung injury. *Am J Pathol* **163**, 2555–2563, 2003.
55. Ogborne RM, Rushworth SA, Charalambos CA, and O'Connell MA: Haem oxygenase-1: a target for dietary antioxidants. *Biochem Soc Trans* **32**, 1003–1005, 2004.
56. Kweon MH, Adhami VM, Lee JS, and Mukhtar H: Constitutive overexpression of Nrf2-dependent heme oxygenase-1 in A549 cells contributes to resistance to apoptosis induced by epigallocatechin 3-gallate. *J Biol Chem* **281**, 33761–33772, 2006.
57. Cornblatt BS, Ye L, Dinkova-Kostova AT, Erb M, Fahey JW, et al.: Preclinical and clinical evaluation of sulforaphane for chemoprevention in the breast. *Carcinogenesis* **28**, 1485–1490, 2007.
58. Yao P, Nussler A, Liu L, Hao L, Song F, et al.: Quercetin protects human hepatocytes from ethanol-derived oxidative stress by inducing heme oxygenase-1 via the MAPK/Nrf2 pathways. *J Hepatol* **47**, 253–261, 2007.
59. Khor TO, Huang MT, Kwon KH, Chan JY, Reddy BS, et al.: Nrf2-deficient mice have an increased susceptibility to dextran sulfate sodium-induced colitis. *Cancer Res* **66**, 11580–11584, 2006.

NUTRITION AND CANCER, 58(1), 75–84

Citrus Auraptene Suppresses Azoxymethane-Induced Colonic Preneoplastic Lesions in C57BL/KsJ-*db/db* Mice

Kei Hayashi, Rikako Suzuki, Shingo Miyamoto, Yoshitani Shin-ichiroh, Hiroyuki Kohno, Shigeyuki Sugie, Shigeki Takashima, and Takuji Tanaka

Abstract: *The current study was designed to investigate whether dietary citrus auraptene (AUR) suppresses the development of azoxymethane (AOM)-induced colorectal preneoplastic lesions in C57BL/KsJ-db/db (db/db) mice with obese and diabetic phenotypes. Female db/db and wild (+/+) mice were divided into the AOM + AUR, AOM alone, AUR alone, and the untreated groups in each phenotype. AOM was given 3 weekly intraperitoneal injections (10 mg/kg bw). AUR (250 ppm) was given in diet during the study (for 10 wk). Dietary AUR significantly reduced the number of aberrant crypt foci (ACF) and β-catenin-accumulated crypt (BCAC) in both phenotypes. The treatment also lowered cell proliferation activity and increased apoptotic cells in both lesions. Our findings indicate that dietary AUR is able to suppress the early phase of colon carcinogenesis in both phenotypes, suggesting possible application of AUR as a chemopreventive agent in both the high-risk and general populations for colorectal cancer.*

Introduction

Numerous epidemiological results suggest that obesity is a risk factor for colon cancer (1,2). There are several studies to investigate possible mechanism for this (3,4). Obesity is a complex, heterogeneous, and multi-factorial syndrome resulting from both genetic susceptibility and environmental factors (5). Besides obesity, it is well known that several factors, including a high fat and low-fiber diet (6), low physical activity (7), inflammatory bowel diseases (8), or hereditary disorders such as familial adenomatous polyposis and non-polyposis syndrome (9), increase the risk for development of colorectal cancer (CRC). For fighting this malignancy, we tried to find natural compounds that are capable to effectively inhibit colon carcinogenesis in a series of pre-clinical studies.

As one of the possible cancer chemopreventive agents, we proposed citrus auraptene (AUR) that is able to inhibit carcinogenesis in various tissues (10–13), including colon (14–17). A prenyloxycoumarin, AUR is a secondary metabolite, mainly found in plants belonging to the families of Rutaceae and Umbelellierae. Several coumarins, including AUR were shown to possess valuable pharmacological properties. These were reported to have anti-inflammatory activity (18). AUR significantly attenuated the lipopolysaccharide-induced protein expression of inducible nitric oxide synthase and cyclooxygenase-2, with decreases in production of nitric anion and prostaglandin E_2, and yet suppressed the release of tumor necrosis factor-α and IκB degradation (19,20). Furthermore, AUR possesses anti-oxidative activity and suppresses lipid peroxidation in rat colon exposed to a colonic carcinogen azoxymethane (AOM) (14,21). AUR is able to induce the activity of detoxifying enzymes without affecting phase I drug metabolizing enzymes in mouse liver (22). In addition, AUR can enhance immune system by affecting macrophage function and cytokine production in mice (23). AUR also suppress experimental lung metastasis of melanoma cells in mice (24). More recently we have found AUR suppresses *β-cetenine* gene mutations in chemically-induced hepatocarcinogenesis in rats (25) and inhibits the expression of matrix metalloproteinase-7 (matrilysin 1), which plays essential roles in cancer progression, in the human colorectal adenocarcinoma cell line HT-29 (26). A variety of biological activities of AUR can be thus responsible for its cancer chemopreventive ability. However, in our series of preclinical chemopreventive studies we used in vitro assays and an experimental animal model, in which colonic carcinogens, such as AOM, were applied to rodents, assuming general population.

C57BL/KsJ-*db/db* (*db/db*) mice are genetically altered models with phenotypes of obesity and diabetes mellitus (27). Disruption of the leptin receptor (Ob-R) gene in the *db/db* mice leads to over-expression of leptin in the adipose tissue and a concomitantly high concentration of leptin in the blood of the mice (28,29). It is widely accepted that leptin

Kei Hayashi, Yoshitani Shin-ichiroh, and Shigeki Takashimaare affiliated with Department of Surgical Oncology, Oncologic Pathology, Kanazawa Medical University, 1-1 Daigaku, Uchinada, Ishikawaa 920-0293. Rikako Suzuki, Shingo Miyamoto, Hiroyuki Kohno, Shigeyuki Sugie, and Takuji Tanaka are affiliated with Department of Oncologic Pathology, Kanazawa Medical University, 1-1 Daigaku, Uchinada, Ishikawaa 920-0293. Shingo Miyamoto is also affiliated with Division of Food Science and Biotechnology, Graduate School of Agriculture, Kyoto University, Kyoto 606-8502, Japan.

functions as a satiety factor through Ob-R, which is mainly expressed in the hypothalamus (29). Because of a deficiency of the leptin-mediated satiety signaling, abnormal dietary habits such as hyperphagia occur in homozygous *db/db* mice, resulting in complex phenotypes. It is now well-established that leptin not only interacts with pathways in the central nervous system, but also functions in the peripheral tissues as a mediator of energy expenditure, a permissive factor for puberty and a signal of metabolic status (30). Interestingly, some lines of evidence suggest that leptin in the periphery behaves as a growth factor in lung (31), breast (32), and colonic tissues (33). Although plausible role of leptin in tumorigenesis remains undetermined, there have been several studies suggesting the leptin-related pathway as a possible modulator in neoplastic development (34–36). We recently reported that the *db/db* mice are susceptible to colon carcinogenesis (3).

In the current study we conducted a short-term assay to examine whether dietary AUR can inhibits the occurrence of AOM-induced preneoplastic lesions, aberrant crypt foci (ACF) (37), and β-catenin-accumulated crypt (BCAC) (38) for CRC in genetically obese *db/db* mice, and compared the effects on +/+ female mice. We also examined the effects of AUR on clinical chemistry in both phenotypes, since certain serum chemistry is related to the occurrence of CRC (39,40). Since modification of cell proliferation activity and apoptosis in the non-lesional and lesional areas in the organ for cancer chemoprevention (41), the effects of AUR on cell proliferation activity and apoptotic index were analyzed immunohistochemically. The main goal of this study was to assess the involvement of obesity-related events such as hyper-leptinemia in colon carcinogenesis and to find promising cancer chemopreventive agents for such a high-risk group of CRC.

Materials and Methods

Animals, Diets, and Carcinogen

Thirty female *db/db* and 30 +/+ mice (4 wk of age) for the study were purchased from the Jackson Laboratories (Bar Harbor, ME). CRF-1 (Oriental Yeast Co., Tokyo, Japan) was used as a basal diet, which consists of 5.7% fat, 22.4% protein, 6.6% minerals, 3.1% fiber, and 62.3% carbohydrate and others (~3.59 kcal/g). The major fatty acids present in CRF-1 were linoleic acid, oleic acid and palmitic acid. AOM was obtained from Sigma (St. Louis, MO). They were housed in a holding room under controlled conditions of a 12 h light/dark cycle, 23 ± 2°C room temperature and 50 ±10% relative humidity. AUR (99.9% purity) was synthesized as described previously (12). Diet containing AUR at a dose level of 250 ppm was made by mixing AUR with powdered CRF-1 every week during the study and stored in the cold room (<4°C). Diets and water during an experimental period were freely available.

Experimental Procedures

Animals of each phenotype was divided into 4 groups: the AOM + AUR group (10 mice), AOM alone group (10 mice), AUR alone group (5 mice), and untreated group (5 mice). They were given 3 weekly intraperitoneal injections of AOM (10 mg/kg body weight). They also fed the AUR-containing diet for 10 wk (entire experimental period). At sacrifice (10 wk after the start of the study), we determined the frequency of ACF and BCAC in the colon. At autopsy, colons of all the mice were removed, cut open longitudinally and fixed in 10% buffered formalin. After removing the rectal sides (2.0 cm from the anus), the colons were cut into two portions (distal and proximal) and the distal colons were used in this study. BCAC was quantified in the rectal mucosa after immunohistochemical staining for β-catenin, and ACF were counted in the remaining parts of the colon that were stained with methylene blue. At autopsy, the weights for pancreas, liver, kidney, and peritoneal adipose tissue were measured.

Counting the Number of Colonic ACF and BCAC

The ACF and BCAC were determined according to the standard procedures that areroutinely used in our and other laboratories (15,38). At necropsy, the colons were flushed with saline, excised, cut open longitudinally along the main axis, and then washed with saline. They were cut, placed on the filter paper their mucosal surface up, and then fixed in 10% buffered formalin for at least 24 h. The fixed colons were stained with methylene blue (0.5% in distilled water) for 20 seconds, dipped in distilled water, and placed on a microscope slide to count the ACF. After counting the ACF, the distal parts (1 cm from the anus) of the colon were cut in order to count the number of BCAC. To identify BCAC intramucosal lesions, the colonic mucosa (mean area: 0.75 cm^2/colon) was embeddedin paraffin, and then a total of 20 serial sections (4 μm thick each) per mouse were made by an *en face* preparation (38). For each case, twoserial sections were used to analyze the BCAC.

Immunohistochemistry for β-Catenin, Cell Proliferation, and Apoptosis

Four serial sections (4 μm thickness) were made from paraffin-embedded blocks. One section was subjected to hematoxylin and eosin (H & E) staining for histopathology and the others for immunohistochemistry of β-catenin, proliferating cell nuclear antigen (PCNA), and apoptosis.

Immunohistochemistry for β-catenin was performed on 4-μm-thick paraffin-embedded sections from the distal segments of the colons, using the labeled streptavidin-biotin method (LSAB Kit; Dako, Glostrup, Denmark) with microwave accentuation. The paraffin-embedded sections were heated for 30 min at 65°C, deparaffinized in xylene, and rehydrated through graded alcohols at room temperature. A 0.05 M Tris-HCl buffer (pH 7.6) was used to prepare solutions and for washes between various steps. The sections were treated for 40 min at room temperature with 2% bovine serum albumin and incubated overnight at 4°C with a primary antibody against β-catenin protein (diluted 1:1000, catalog no. 610154, BD Transduction Laboratories, Lexington, KY). Horseradish peroxidase activity was visualized by treatment

with H_2O_2 and diaminobenzidine for 5 min. Negative control sections were immunostained without the primary antibody. Immunoreactivity was regarded as positive if apparent staining was detected in the cytoplasm and/or nuclei to determine the BCAC.

For PCNA immunohistochemistry, formalin-fixed, paraffin-embedded distal colon sections were subjected to deparaffinization and dehydration prior to quenching of endogenous peroxidase activity (1.5% H_2O_2 in methanol for 20 min). An antigen-unmasking step was done by placing the slides in a pressure cooker containing 0.01 M sodium citrate (pH 6.0) for 10 min. The sections were incubated for 60 min with the primary mouse anti-rat PCNA monoclonal antibody (Clone PC-10, DakoCytomation, Cat no. M0879) at a dilution of 1:1500 in 10% goat serum. Secondary antibody, biotinylated goat anti-mouse IgG (Cat no. BA-2000, Vector Laboratories, Burlingame, CA) was applied for 30 min in a 1:500 dilution. Slides were processed with the ABC reagent from Vectastain Elite (Vector Laboratories) using DAB as the substrate. Sections were counterstained with hematoxylin. In the distal colonic mucosa without lesions from 5 mice of each group, 20 fields, randomly selected from each slide, were analyzed at ×400 magnification. PCNA-positive cell nuclei were determined in 10 ACF each from the AOM + AUR and AOM alone groups of each phenotype. Also, PCNA-positive cell nuclei were analyzed in 5 BCAC from the AOM + AUR group and 12 BCAC from the AOM alone group from each phenotype. Cells staining positive for PCNA were scored as a percentage of total cells in each field or lesion.

Levels of apoptosis in distal colon tissue were determined by the TdT-mediated dUTP nick-end labeling (TUNEL) method. Four-μm formalin-fixed, paraffin-embedded tissue sections from the distal colons were processed according to manufacturer's instructions using Apoptosis in situ Detection Kit Wako (Cat. No. 298-60201, Wako Pure Chemical Industries, Ltd., Osaka, Japan). The kit is based on TUNEL procedure. Appropriate positive and negative controls for determining the specificity of staining were generated. Negative controls were processed in the absence of the terminal deoxynucleotidyl transferase (TdT) enzyme in the reaction buffer. Sections of colon tissue digested with nuclease enzyme and colon lymphoid nodules, which are known to exhibit high rates of apoptosis, were used as positive controls. Color was developed with the peroxidase substrate DAB, and sections were counterstained with hematoxylin. For each section, 20 fields of normal-appearing tissue were randomly selected and photographed at ×400 magnification. The numbers of apoptotic cells per field of normal mucosa from 5 mice of each group of both phenotypes were counted and recorded as a percentage of total cells in each field or lesion. Also, randomly chosen 10 ACF each from the AOM + AUR and AOM alone groups, 5 BCAC each from the AOM + AUR group of both phenotypes, and 12 BCAC each from the AOM group of both phenotypes were counted for apoptosis. The apoptotic index was calculated by dividing the total number of apoptotic cells by the number of atypical cells that consist of ACF or BCAC, and was expressed the percentage.

Measurement of Serum Glucose, Leptin, Total Cholesterol, and Triglycerides Levels

At sacrifice, blood to measure the serum concentrations of glucose, leptin, total cholesterol, and triglycerides was collected from all mice each of genotypes. They were starved overnight prior to blood collection for clinical chemistry. The serum glucose level was measured enzymatically using the hexokinase method. The serum triglycerides were assayed by enzymatic hydrolysis with lipase. Serum cholesterol was determined enzymatically using cholesterol esterase and cholesterol oxidase. Serum concentration of leptin was measured by an enzyme immunoassay according to the manufacturer's protocol (R&D Systems, Minneapolis, MN).

Statistical Analysis

Where applicable, data were analyzed using Tukey-Kramer multiple comparison test (GraphPad Instat version 3.05, GraphPad Software, San Diego, CA) with $P < 0.05$ as the criterion of significance.

Results

General Observation

Mean daily intakes of diet of mice of all groups in the *db/db* mice were about 1.30 times greater than those of the +/+ mice. Dietary feeding with AUR did not cause clinical symptoms including toxicity in each phenotype. The mean body, liver, kidney, and peritoneal adipose tissue weights in all groups of *db/db* mice were significantly greater than those of respective groups of +/+ mice, regardless of treatment ($P < 0.001$ for each comparison, data not shown). In the *db/db* mice, the mean body weight in the AOM + AUR group (39.6 ± 3.8 g, $P < 0.01$) was significantly lower than that of the AOM group (44.0 ± 1.7 g). The mean pancreas weights of the AOM + AUR, AOM alone, and untreated groups of *db/db* mice were relatively lower than +/+ mice without statistical significance. Interestingly, the pancreas ($P < 0.001$) weight in the AOM + AUR group (0.13 ± 0.02 g, $P < 0.001$) of the *db/db* mice were significantly lower than that of the AOM group (0.18 ± 0.03 g). The mean weights for liver, kidney, and peritoneal fat tissue did not significantly differ among the groups of the *db/db* mice. Dietary administration of AUR did not affect the weights of body, liver, kidney, pancreas, and peritoneal fat tissue in the +/+ mice.

Frequencies of ACF and BCAC

Data on ACF (Fig. 1A and B) counting are listed in Table 1. ACF developed in *db/db* and +/+ mice that received AOM injections, and the value of the AOM alone group was significantly greater in *db/db* mice when compared to that of +/+ mice ($P < 0.001$). Dietary feeding with AUR significantly lowered the numbers of total ACF and large ACF with 4 or more crypts in the *db/db* mice ($P < 0.001$) and +/+ mice ($P < 0.001$) when compared to those of the AOM

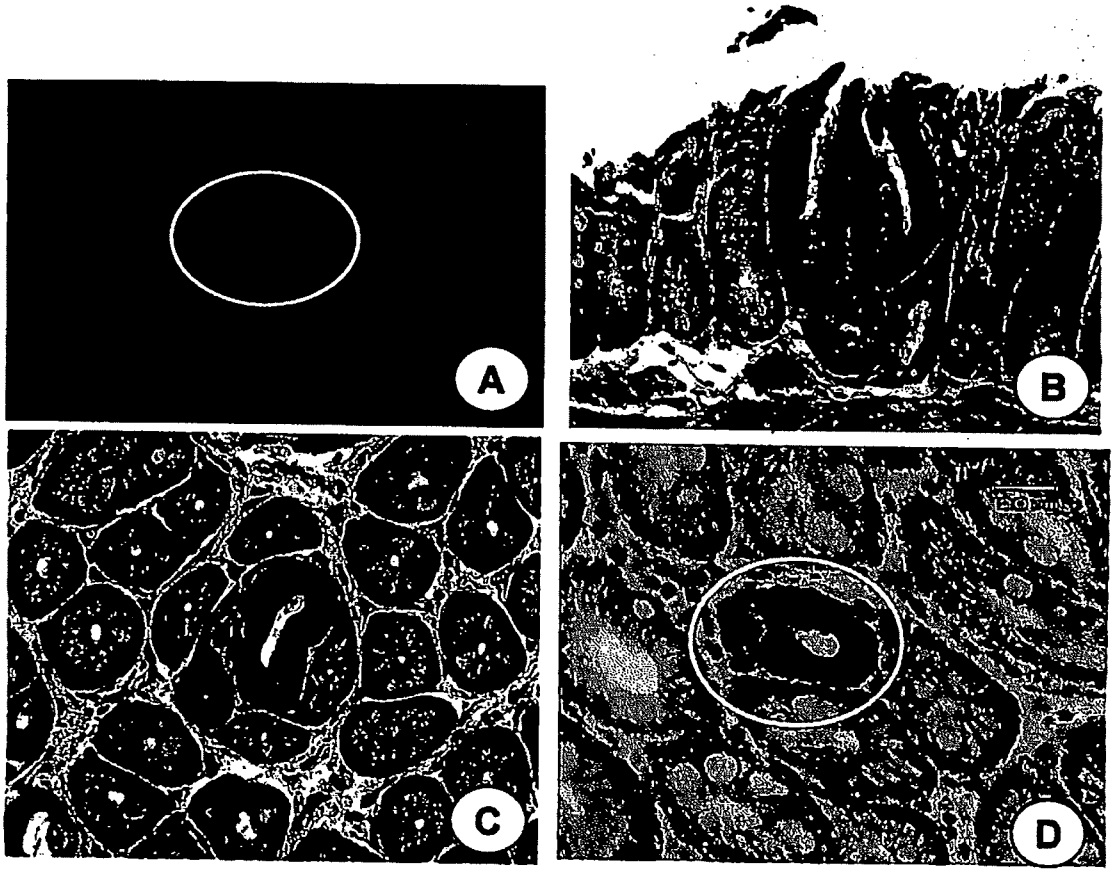

Figure 1. Morphology of preneoplastic lesions, ACF and BCAC, for CRC in the *db/db* mice that received AOM. (A) a large ACF (circled) consists of 4 aberrant crypts is observed methylene-blue stained colonic mucosa; (B) Histopathology of an ACF consists of 2 aberrant crypts in H& E-stained section; (C) a BCAC (circled) found in H & E-stained section. Cells in a BCAC have relatively large and hyperchromatic nuclei with mitoses; and (D) a BCAC found in the section of β-catenin immunohistochemistry. Cells in BCAC strongly express immunoreactivity for β-catenin in their cell membrane, cytoplasm, and some nuclei. Original magnification: (A) ×4; (B) ×10; (C) ×10; and (D) ×20.

alone group. Similarly the number of BCAC (Fig. 1C and D) in the AOM alone group of *db/db* mice was larger than that of the +/+ mice ($P < 0.05$), as shown in Fig. 2. The values of the AOM + AUR group of both phenotypes were significantly smaller than those of the AOM alone group ($P < 0.001$ for the *db/db* mice and $P < 0.01$ for the +/+ mice). ACF and BCAC were not present in the AUR alone and untreated groups of each phenotype.

PCNA-Labeling Index

As shown in Fig. 3A, PCNA-labeling index of non-lesional crypts in the *db/db* mice was greater than that of +/+ mice, regardless of the treatment: the labeling indices of the AOM alone and AOM + AUR groups were significantly larger than those in +/+ mice ($P < 0.001$ and $P < 0.01$, respectively). In the *db/db* mice, the index of the AOM + AUR group was significantly smaller than that of the AOM alone group ($P < 0.01$). The PCNA labeling index of ACF of the AOM alone group in the *db/db* mice was significantly larger than that of +/+ mice (Fig. 3B, $P < 0.05$). AUR feeding significantly lowered the index in the *db/db* mice ($P < 0.05$). As for the PCNA labeling index of BCAC, feeding with AUR significantly reduced the index in both the +/+ and *db/db* mice (Fig. 3C, $P < 0.001$).

Apoptotic Index

The data on the apoptotic index of non-lesional crypts, ACF, and BCAC are illustrated in Fig. 4. The apoptotic index of the non-lesional crypts of the AOM alone group in the *db/db* mice was significantly larger than that of +/+ mice (Fig. 4A, $P < 0.05$). In the AOM + AUR group of the *db/db* mice was significantly smaller than that of the AOM alone group (Fig. 4A, $P < 0.001$ each). AUR feeding significantly elevated the index of ACF that developed in both the phenotypes (Fig. 4B, $P < 0.001$). Also, the index of BCAC in the AOM + AUR group was significantly higher than that of the AOM alone group of both the phenotypes (Fig. 4C, $P < 0.001$ each).

Table 1. Effect of auraptene on the development of ACF induced by AOM.

Phenotype	Treatment (number of mouse examined)	Total ACF/colon	1 crypt	2 crypts	3 crypts	4 or more crypts	Total ACs/colon
db/db	AOM→250 ppm AUR (10)	30.6±8.7	7.5±2.7	7.4±2.6	8.4±2.4	7.3±2.3	84.3±24.2
		(p<0.001)	(p<0.001)		(p<0.001)	(p<0.001)	(p<0.001)
	AOM alone (10)	80.4±14.6	14.0±3.2	11.7±3.0	17.2±4.0	37.5±6.9	294.3±53.1
		(p<0.001)			(p<0.001)	(p<0.001)	(p<0.001)
	250 ppm AUR (5)	0	0	0	0	0	0
	None (5)	0	0	0	0	0	0
Wild	AOM→250 ppm AUR (10)	29.1±8.2	7.7±2.0	7.8±3.3	6.1±2.1	7.5±4.1	78.7±30.8
		(p<0.001)	(p<0.01)	(p<0.05)	(p<0.01)	(p<0.001)	(p<0.001)
	AOM alone (9)	58.8±6.8	12.6±2.2	13.3±5.1	11.0±2.6	21.9±2.5	193.2±24.0
	250 ppm AUR (4)	0	0	0	0	0	0
	None (5)	0	0	0	0	0	0

Statistical analysis was done by ANOVA, Tukey-Kramer multiple comparison test.

Serum Levels of Total Cholesterol, Triglycerides, Glucose, and Leptin

As illustrated in Fig. 5, all the measurements (total cholesterol, triglycerides, glucose, and leptin) were significantly larger in the *db/db* mice than in the +/+ mice ($P < 0.001$ or $P < 0.01$). Among the measurements in the *db/db* mice, serum concentration of triglycerides in the AOM + AUR group was significantly smaller than that of the AOM alone group ($P < 0.01$, Fig. 5B). Also, the value of the AUR alone group was significantly lower than that of the untreated group ($P < 0.001$, Fig. 5B). Dietary AUR did not affect the chemical profiles other than triglycerides measured in the *db/db* mice (Fig. 5A, C, and D). In the +/+ mice, there were no significant differences on all the measurements among the groups (Fig. 5A, B, C, and D).

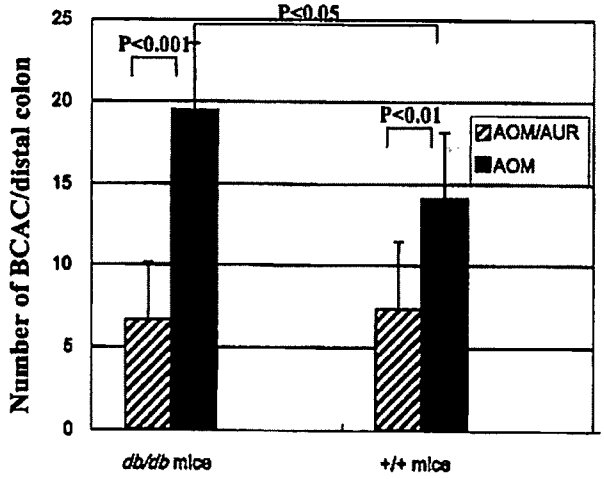

Figure 2. Frequencies of BCAC in the AOM + AUR and AOM alone groups in the *db/db* and +/+ mice. The frequency of the AOM group is significantly greater in the *db/db* mice than in the +/+ mice ($P < 0.05$). Dietary feeding with AUR significantly reduced the frequency in both phenotypes ($P < 0.001$ for the *db/db* mice and $P < 0.01$ for the +/+ mice).

Discussion

Our results in the current study clearly indicated that dietary AUR is able to suppress the development of precursor lesions, ACF and BCAC, for CRC in obese mice as well as wild type mice. The inhibition is considered to be cause by lowering serum triglycerides, inducing apoptosis, and/or reducing cell proliferation. In addition, the results of the current study confirmed the high susceptibility of the obese/diabetic *db/db* mice to AOM-induced colon carcinogenesis (3,42).

The high susceptibility in the *db/db* mice might be related to the increases in the high cell proliferation activity in the non-lesional crypts (Fig. 4A) that may be related obese and high levels of serum cholesterol, triglycerides, glucose, insulin, and leptin, thus suggesting a positive association